

**Santa Clara University
Scholar Commons**

Mechanical Engineering Senior Theses

Engineering Senior Theses

6-2018

Active Control Stabilization of High Power Rocket

Valeria Avila Guerrero

Santa Clara University, vavilaguerro@scu.edu

Angel Barranco

abarranco@scu.edu

Daniel Conde

Santa Clara University, dconde@scu.edu

Follow this and additional works at: https://scholarcommons.scu.edu/mech_senior



Part of the [Mechanical Engineering Commons](#)

Recommended Citation

Guerrero, Valeria Avila; Barranco, Angel; and Conde, Daniel, "Active Control Stabilization of High Power Rocket" (2018). *Mechanical Engineering Senior Theses*. 81.

https://scholarcommons.scu.edu/mech_senior/81

This Thesis is brought to you for free and open access by the Engineering Senior Theses at Scholar Commons. It has been accepted for inclusion in Mechanical Engineering Senior Theses by an authorized administrator of Scholar Commons. For more information, please contact rscroggin@scu.edu.

SANTA CLARA UNIVERSITY

Department of Mechanical Engineering

I HEREBY RECOMMEND THAT THE THESIS PREPARED
UNDER MY SUPERVISION BY

Valeria Avila Guerrero, Angel Barranco, Daniel Conde

ENTITLED:
**ACTIVE CONTROL STABILIZATION OF HIGH POWER
ROCKET**

BE ACCEPTED IN PARTIAL FULFILLMENT OF THE REQUIREMENTS
FOR THE DEGREE OF
BACHELOR OF SCIENCE
IN
MECHANICAL ENGINEERING

M. A. Ayoubi

Thesis Advisor, Dr. Mohammad Ayoubi

06/13/2018

Date

T. E. Shoup

Department Chair, Dr. Terry Shoup

6/14/18

Date

ACTIVE CONTROL STABILIZATION OF HIGH POWER ROCKET

By

Valeria Avila, Angel Barranco, Daniel Conde

SENIOR DESIGN PROJECT REPORT

Submitted to

The Department of Mechanical Engineering

of

SANTA CLARA UNIVERSITY

in Partial Fulfillment of the Requirements

for the degree of

Bachelor of Science in Mechanical Engineering

Santa Clara, CA

2018

Contents

Contents	iii
List of Figures	v
List of Tables	vii
1 International Traffic of Arms Regulations Disclaimer	viii
2 Abstract	1
3 Introduction	2
4 Systems Level	3
5 Preliminary Rocket Design	7
5.1 Sizing of Engine Motor to Determine Body Dimensions	7
6 Rocket Design Geometry	9
6.1 Canards	10
6.2 Final Design	12
7 Modeling and Analysis	13
7.1 Static Stability	13
7.2 Dynamic Stability	16
7.3 Finite Element Analysis: Mode Shapes	20
7.4 Drag Coefficient and Digital DATCOM	22
7.5 Computational Fluid Dynamics	25
8 Flight Dynamics	26
8.1 Six Degrees-of-Freedom (6DOF) Mathematical Model	26
8.2 Simulation Results	33
8.3 Control System Design Via LQR	34

9 Electronics Bay Design	37
9.1 Previous Projects	37
9.2 Conceptual Design	38
9.2.1 Servo Motors	39
9.2.2 Altimeter Data Logging	41
9.3 Prototype	41
10 Summary and Conclusions	44
11 Appendices	A-1
11.1 Appendix A: Market Research Findings	A-1
11.2 Appendix B: Project Design Requirements PDS	B-1
11.3 Appendix C: Assembly Drawings	C-1
11.4 Appendix D: Senior Design Conference Presentation Slides	D-1
11.5 Appendix E: Gantt Chart	E-1
11.6 Appendix F: Business Plan	F-1

List of Figures

1	Sounding rockets size chart.	2
2	Illustration of user interaction with the device.	6
3	Subsystems and their interaction with each other	7
4	Results from solving rocket equation without drag.	8
5	Plot of altitude versus time during coasting phase.	9
6	Initial CAD model.	10
7	CAD model of the canard fin design.	11
8	Differences between airfoil shapes.	12
9	3D model of final rocket design.	12
10	Underdamped homogeneous response of the rocket.	19
11	Underdamped step response of the rocket.	19
12	Deformation of the rocket at a 0.21 Hz resonant frequency of Mode 5.	21
13	Mode shape results.	21
14	DATCOM Model.	24
15	Fluid flow around one canard fin.	25
16	Fluid flow around the entire body at maximum velocity.	25
17	Inertial frame and its relationship to the structure frame and body frame.	27
18	Body rates shown in the body frame.	28
19	Forces acting on body shown in the body frame.	30
20	Altitude versus time acquired by the 6DOF simulation.	33
21	Angular rates versus time acquired by the 6DOF simulation.	33
22	Adriano Arcadipane's payload design	37
23	Rendering of preliminary concept design	38
24	First payload prototype	39
25	Plot of generic first order response under a unit step input. Figure depicted by Valeria Avila.	40
26	First control system prototype using Arduino and MPU6050 gyroscope.	41
27	Schematic of the connections between the components of the circuit	42

28	Latest iteration of the payload without canards installed.	43
29	Payload enclosed with fiberglass coupler	44

List of Tables

1	Sample data found from the interview with Paul Reed.	4
2	Interpretation of data acquired from interview.	5
3	Natural frequencies for the first six modes of the rocket.	20

1 International Traffic of Arms Regulations Disclaimer

Due to ITAR Defense regulations, the information detailed in this thesis will not be exported outside of the continental US according to ITAR Regulations 121.1, Category 4, paragraph H: (1) Flight control and guidance systems (including guidance sets) specially designed for articles enumerated in paragraph (a) of this category (MT for those articles enumerated in paragraphs (a)(1) and (a)(2) of this category);

Note to paragraph (h)(1): A guidance set integrates the process of measuring and computing a vehicle's position and velocity (i.e., navigation) with that of computing and sending commands to the vehicle's flight control systems to correct the trajectory.

This system is not designed nor intended to be used as a weapon, rather stabilizing a high-power sport rocket flying vertical. The project intentions are for educational and research purposes.

2 Abstract

High power rockets could become dynamically unstable due to outside disturbances after take-off. The instability is augmented when the rocket is "slow" off the launch rail, which happens when the thrust-to-weight ratio is less than 5:1. Due to these reasons, the objective of this project was to design and build an active control system that will make sure the rocket follows a straight path all the way to apogee. This will be done through a model-based design approach, in which a 6DOF mathematical model of the flight dynamics will be created.

3 Introduction

Motivation and Background

High-power rocketry – a hobby popularized in the late 1950's after Sputnik's launch – is similar to model rocketry. The major difference between the two, however, is that higher impulse range motors are used. The National Fire Protection Association (NFPA) defines a high-power rocket as one that has a total weight of more than 1,500 grams and contains a motor or motors containing more than 125 grams of propellant and/or rated at more than 160 Newton-seconds of total impulse. Figure 1¹ compares different sounding rockets' sizes; our rocket would be located at the leftmost side of the chart.

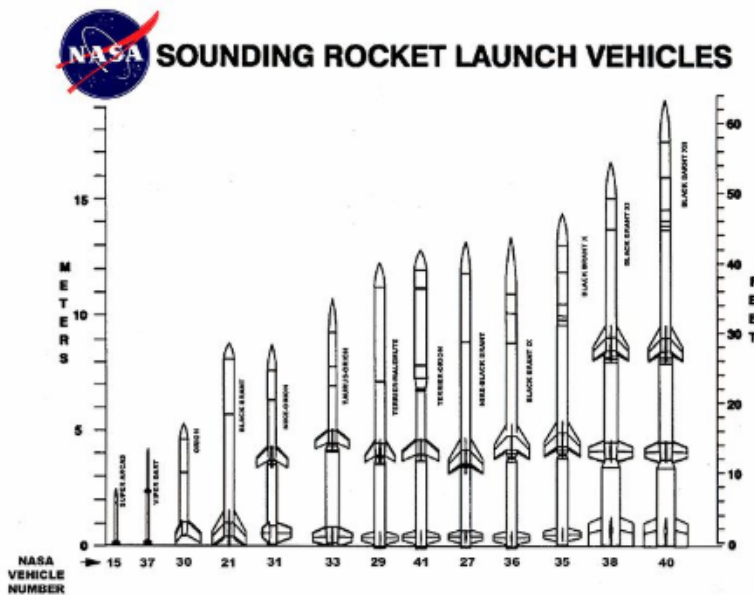


Figure 1: Sounding rockets size chart.

Outside disturbances could make such high-power rockets dynamically unstable, causing it to deviate from its desired flight path or destroy itself. An example of the behavior due to disturbances is weathercocking, which happens when the rocket has a low-thrust-to-weight ratio (5:1) and flies at a low velocity from the launch rail. This causes the rocket to turn towards the wind's direction. One way to make these rockets dynamic stable is by roll stabilization, which essentially involves making the rocket spin at high RPM along its longitudinal axis to create

¹<https://www.wff.nasa.gov/code810/vehicles.html>

a high moment of inertia capable of resisting outside disturbances. However, this method is found to be undesirable because sensors may struggle recording data and undisturbed footage of the ascent flight is desirable in most cases. The purpose of this project is to design an ascent flight control system for high-power rockets that will actively stabilize a rocket's attitude, so that it remains within 5 degrees from the ascent flight path while reaching a maximum altitude of 3,000 [m]. Such constraint was used because according to safety regulations imposed by the National Association of Rocketry (NAR), multistage projects require that rockets remain within 5 degrees from the vertical position. Moreover, both the pitching and yawing motion will be kept at less than 0.01 rad/s in order to minimize the weathercocking effects. Lastly, this control system will eliminate the natural rolling motion of rockets, making it possible for ascent footage to be captured.

4 Systems Level

Customer Needs

Key populations were interviewed in this project: Hobbyists, educators, and researchers. Slow rockets are defined as having a thrust-to-weight ratio between 1 and 3. Since an adequate velocity is not achieved before leaving the launch rail, the wind encountered easily causes the rocket to deviate from its vertical path; therefore, the control system must correct and/or prevent such deviations. This specific need is very important because, as many interviewed customers noted, hobbyists design multi-stage rockets, and for such projects it is required that the rocket stay within a tight band of < 5 degrees from the vertical axis for safety reasons. Moving on, another need is that the control system must eliminate roll because of the desire to capture footage of the ascent flight. The last major need is that the control system must be light enough, so that no significant weight is added to the payload. Related to the mass of the system is its size; the control system must fit in a typical size for high-power rockets, which start at a minimum diameter of about 3 inches. Current products similar to the project were researched, but there are no examples commercially available potentially due to ITAR regulations. Table 1 shows relevant findings on the preliminary assessment from an interview with Paul Reed, a hobbyist

Table 1: Sample data found from the interview with Paul Reed.

Customer:	Paul Reed	Interviewer:	Valeria
Affiliation:	Tulsa Rocketry	Date:	10/23/17
Contact Info:	trprefect@gmail.com	Type of User	Hobbyist, Educator
Questions/Prompt	Customer Statement	Interpreted Need	
Applications of an active stabilization system	The rocket going straight up because of multi-stage projects; no roll is desired because of camera on board	Rocket flies vertically	
		No roll to capture footage	
Type of payload required?	Any system needs to fit within the existing air frames sizes in high power rocketry	Payload fits within commercially used sizes	
	The system needs to be light to achieve maximum altitude	Light payload to keep mass low	
Type of stabilization (roll, yaw, pitch)	Many rockets have cameras installed to capture the ascent flight with no roll	Rolling motion eliminated and vertical flight	
Accuracy	Due to safety reason, many multi-stage projects are required to stay within < 5 degrees from the vertical	Rocket stays within 5 deg. from vertical axis	

and educator; its general interpretations to customers needs shown in Table 2. Needs im-

portance hierarchy is shown with primary needs listed in bold, secondary listed below. Importance rating is shown with asterisks (** being the highest) and latent need with exclamation mark (!).

Table 2: Interpretation of data acquired from interview.

Hierarchy	Need
***	Rocket is stabilized once it leaves launch rail, even at low speed
**	Stabilization works with low thrust-to-weight ratios (3:1)
***	No rolling motion
***	Rocket flies vertically
*	Rocket's stabilization stays within < 5 degrees from the vertical axis
***	Actively stabilized through ascent
!	Rocket is stabilized no less than previous designs with fin stabilization
!	Rocket's stabilization achieves maximum altitude possible wrt its mass
*	Stabilization agrees with payload purpose
**	Rocket provides stable platform to take pictures/video
***	Payload fits within commonly used sizes in high power rocketry
***	Payload is light and does not add significant mass to the system
*	System's cost agrees with the efficacy and cost
**	Active stabilization system cost lies under the cost of existing systems such as in Multitronix.

At the end of this market analysis, the most appropriate end user are hobbyists and potential researchers who look for improved flight performance. Therefore, the design requirements defining this project are based on standards for high power rocketry competitions.

Project design requirements (PDS) were defined and seen in detail in Appendix B.

The project is best outlined with the following user scenario in which the person using the rocket studies its flight performance once the system is installed. Figure 2 best explains the

user scenario that hobbyists experience. The customer's rocket is positioned in the launch raid and the electronics are turned on. The rocket is launched and recovered per rocket motor's specification. Later, the retrieved data from the payload can be analyzed in a computer.



Figure 2: Illustration of user interaction with the device.

Functional Analysis

The different subsystems that compose the project are: control system, the electronics payload and canard fins, the rocket body and the propulsions system. Figure 3 illustrates the interconnection between these systems. The battery will be powering the electronics bay, which houses the control system. Once the motor is ignited, the rocket will experience aerodynamic forces, which in turn cause moments about the rocket's center of mass. It is when the control systems adjust the canard fins to make sure the rocket does not roll and it stays within its desired flight path. This will be achieved with the help of sensors that will provide information to the control system via a feedback-loop. Those sensors will tell the control system when apogee has been reached, which will then deploy the parachute in order to safely recover the rocket.

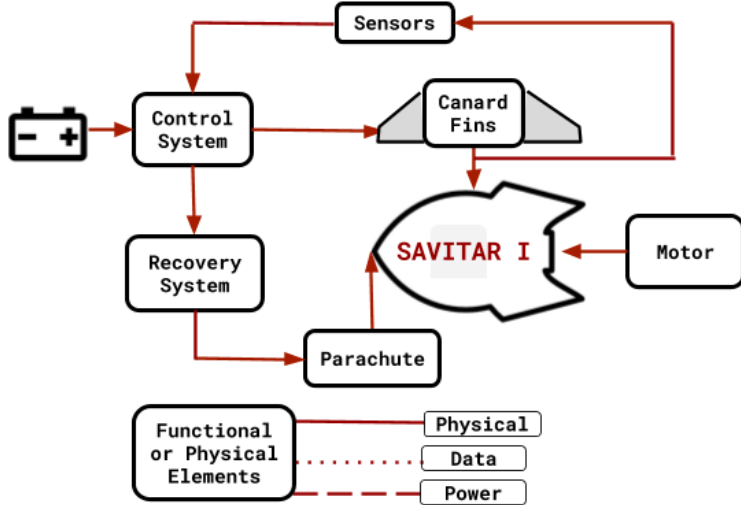


Figure 3: Subsystems and their interaction with each other

5 Preliminary Rocket Design

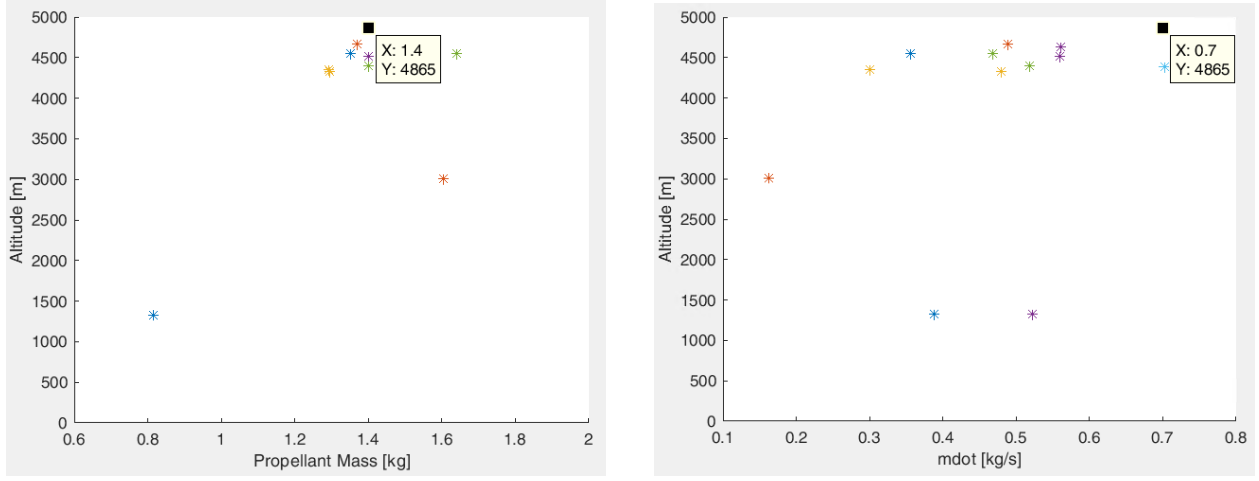
5.1 Sizing of Engine Motor to Determine Body Dimensions

To get a preliminary size of the motor to satisfy the altitude requirement of 3,000 m, a form of the rocket equation without drag was implemented for a particle model:

$$h_{max} = \frac{1}{2} g_0 I_{sp}^2 \ln^2 \left(\frac{m_0}{m_f} \right) - \frac{g_0 I_{sp}}{\dot{m}_e} \ln \left(\frac{m_0}{m_f} \right) + \frac{I_{sp} g_0}{\dot{m}_e} (m_0 - m_f), \quad (1)$$

where g_0 is the acceleration due to gravity at sea level, I_{sp} is the specific impulse of the motor, m_0 is the rocket mass just before launch, m_f is the rocket mass after burnout, and \dot{m}_e is the rate of change of propellant mass. Eq. 1 computes the maximum theoretical height that a rocket can achieve given parameters for a specific motor. In addition, it must be noted that in this particle model, drag is not considered in Eq. 1, therefore no geometric parameters for the rocket are needed. Through an iterative process done in Matlab, the theoretical altitude for a set of 57 motors was calculated given their parameters. To choose a suitable motor, the maximum altitude was plotted versus the propellant mass m_e and its mass flow rate, \dot{m}_e as shown in Figure 4 and 5.

Based on Figure 4, the L1100 motor was chosen because it reached a maximum altitude of 4,865 [m] and had one of the highest mass flow rates 1.4 [kg/s]. After choosing the motor,



(a) Altitude versus propellant mass.

(b) Altitude versus rate of change of propellant mass.

Figure 4: Results from solving rocket equation without drag.

a body diameter of 4 inches 10.12 [cm] was chosen. Factors that contributed in deciding this diameter were payload geometry limitations and rocket kit availability. At 4 inches, the body tube is large enough to accommodate all the control system hardware. In addition, rocket kits of this body dimension are commercially available; this would make it easier for the team to obtain a rocket kit from any vendor. Once the diameter of the body was chosen, the coefficient of drag and cross-sectional area were calculated. The equations for determining the drag coefficient and frontal area are listed in Section 5.5. Knowing the coefficient of drag, a form of the rocket equation with drag was then implemented; the form used is as follows:

$$\begin{cases} \dot{V} = I_{sp} g_0 \frac{\dot{m}_e}{m_0 - \dot{m}_e t} - \frac{1}{2} \rho C_D A \frac{V^2}{m_0 - \dot{m}_e t} - g_0 \sin(\gamma) & 0 \leq t \leq t_{burn} \\ \dot{h} = V \sin(\gamma) & 0 \leq t_{apogee} \end{cases}, \quad (2)$$

$$\begin{cases} \dot{V} = -\frac{1}{2} \rho C_D A \frac{V^2}{m_0 - \dot{m}_e t} - g_0 \sin(\gamma) & t_{burn} \leq t \leq t_{apogee} \\ \dot{h} = V \sin(\gamma) & 0 \leq t_{apogee} \end{cases}. \quad (3)$$

Eq.2 is first evaluated from the time of ignition to the time after burnout, which for the motor selected is 2 [s]. On the other hand, Eq.3 is evaluated during the coasting phase, which is after burnout until reaching apogee. Using Matlab® ODE45 solver, the piecewise function was solved numerically and the results are shown below.

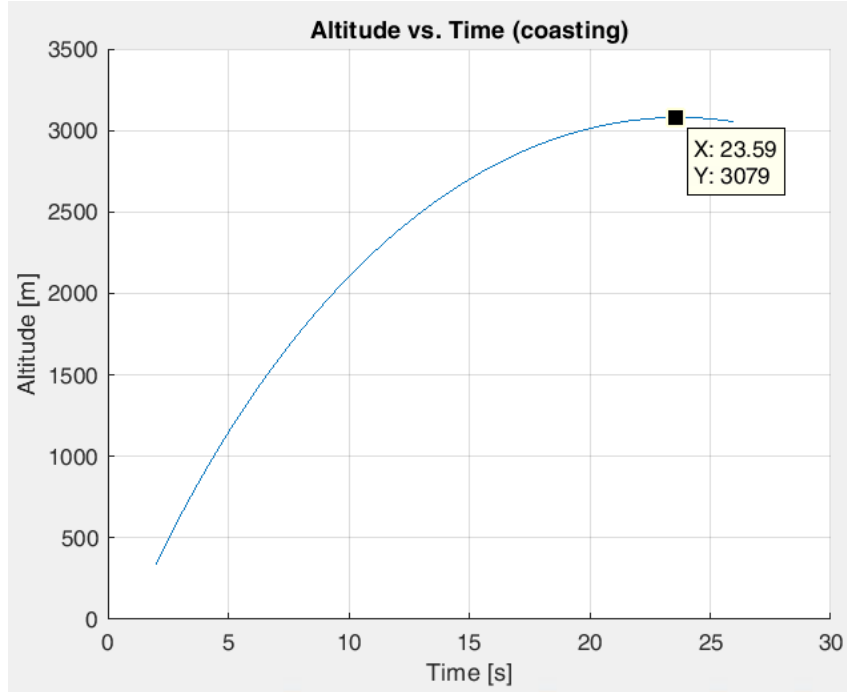


Figure 5: Plot of altitude versus time during coasting phase.

As Figure 5 shows, the maximum altitude is about 3,079 [m], which is just above the altitude target. Based on this result, it was concluded that the AeroTech L1110 is, indeed, the right motor for our purposes.

6 Rocket Design Geometry

As previously mentioned, the rest of the rocket geometric parameters were determined based on the body diameter. Multiple mediums and techniques were implemented in order to find a working design. The techniques implemented included using geometric relationships in literature, particularly from Gordon K. Mandell in *Topics in Advanced Model Rocketry*. A Matlab program was also implemented, relating static stability and geometry. Lastly, the use of open source software *OpenRocket* for model rocket design and launch simulation contributed into the calculations verification. However, inconsistent results failed to infer a reliable solution; therefore, assumptions and approximations were implemented discussed in detail under *assumptions*.

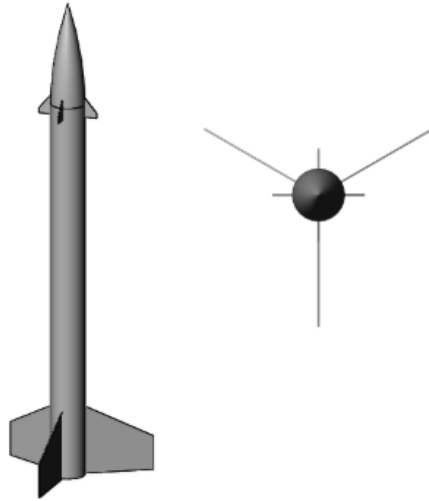


Figure 6: Initial CAD model.

The main goal to achieve with these dimensions is for the rocket to be statically stable by maintaining a static margin stability between 1 and 2 body calibers. Static margin stability being the distance between the center of gravity and center of pressure in terms of body calibers, or body diameters. This value is used to characterize the static longitudinal stability and controllability of aircraft and missiles. This range ensures control over the rocket's trajectory to maintain stability and avoid serious disturbances later studied during control system design phase.

Other than the stability design constraint, drag reduction is the main concern to maximize flight altitude. The dimensions of the chosen rocket components and manufacturing of the canard fins is described in the following sections

6.1 Canards

The canard fins are additional fins added to the body of the rocket after and in front of the tail fins. In aeronautics, canards perform various functions, from lift induction and drag reduction to improvement in stability and/or aircraft control. For our project, the canard fins' primary purpose is to serve as control surfaces directed by our control system that minimize unintentional oscillation the rocket experiences during flight. The gyroscope of the control system assesses the orientation of the rocket, and the control system uses the servos to adjust the canard

fins to counteract rolling, yawing, or pitching of the rocket.

The canard fins of the rocket use a symmetrical clipped delta airfoil shape design. General delta wings and fins resemble the shape of right triangles, with the trailing edge of the fin being perpendicular to its root edge; however, a clipped delta fin has the lower corner trimmed off, as shown in Figure 7.

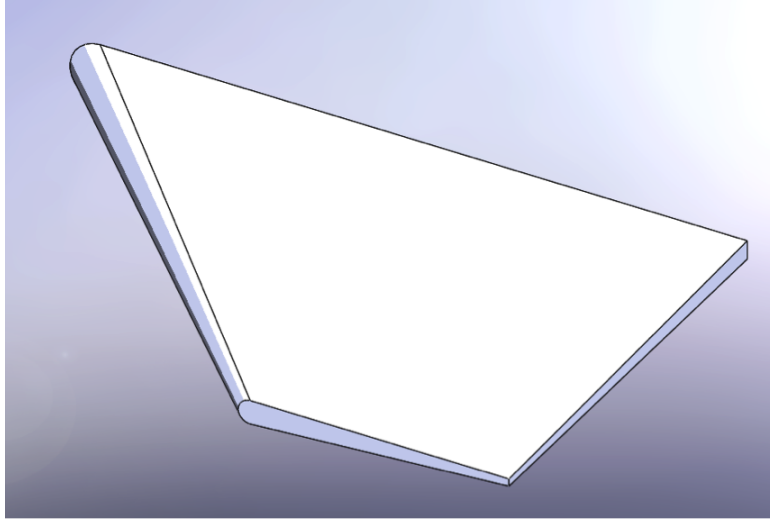


Figure 7: CAD model of the canard fin design.

The actual purpose of this swept edge is to move the shockwave very high-powered rockets experience after going supersonic, but since our rocket does not ever achieve supersonic speeds, the cut is instead used to help reduce weight of the canards and minimize overall load on the shafts that connect the canards to the control system. The reasoning behind a clipped delta design for our canard fins was to help reduce the amount of drag on the rocket. In an issue published by Apogee Rockets, a simulation for a subsonic rocket using various fin shapes was conducted, and it was concluded that the clipped delta fin experienced the lowest drag at a zero-degree angle of attack².

There are a few differences between a typical symmetrical clipped delta fin airfoil and our airfoil. Our rocket's canards have a more rounded leading edge than a typical symmetrical clipped delta fin. In addition, bulk of the canard fin is placed towards the front at the leading edge instead of the fin's center. Furthermore, our airfoil profile tapered straight towards the

²Peak of Flight Newsletter, Issue 442, entitled "What is the best fin shape for a model rocket?", by Apogee Rockets.

trailing edge, while the standard clipped delta fin is more curved and swept aft. Finally, the trailing edge of our delta fin is left a straight edge, while the typical symmetrical design has a sharpened edge. These differences can be seen in the side profile views of both airfoil designs, as shown below in Figure 8.



Figure 8: Differences between airfoil shapes.

These differences made in our canard fins' airfoil shape were primarily because of the trouble in creating the canard fins from scratch. Due to the difficulty in manufacturing an almost perfectly symmetrical airfoil, we 3D printed the canard fins for our rocket. We found that a sharpened trailing edge on the canard fins would break off easily, which is the reason for having a straight trailing edge instead. We also learned that due to the way plastic is layered in 3D printing, creating an airfoil with a profile that is swept aft causes bumps on the surface of the fin where fin thickness is small. As a result, we instead created canard fins with a straight, tapered profile and with the leading edges being the thickest part of the fins.

6.2 Final Design

Once all the dimensions for the body parts were determined, a CAD model was constructed to show how all the components were going to be assembled together.

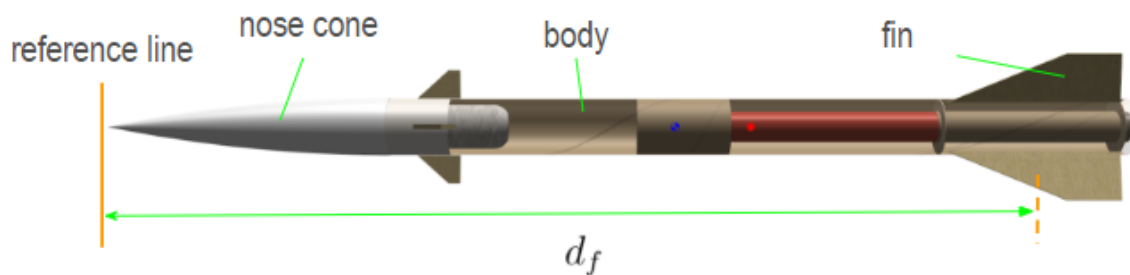


Figure 9: 3D model of final rocket design.

7 Modeling and Analysis

7.1 Static Stability

The static stability of a rocket can be defined as the tendency for a rocket to return to its original intended flight path after launch. What determines a rocket's static stability are its locations for its center of gravity and center of pressure on its body. As the rocket is in flight, force from the wind and a moment arm created by the center of gravity and center of pressure cause the rocket to rotate around its center of gravity. The behavior of the rocket and how it rotates in response to the wind is best described by the rocket's static stability margin.

The rocket's static stability margin is defined as the ratio between the distance from its center of gravity to center of pressure and the body diameter of the rocket. Typically, a rocket with a high static stability (≥ 1) margin tends to be more stable than one with a low static stability margin (< 1). However, for this project, as stated earlier, the goal was to design a rocket that met competition guidelines and had a stability margin between 1.0 and 2.0. Determining both the rocket's center of gravity and center of pressure were based on the individual components that made up the aerostructure of the rocket.

Center of Gravity

The rocket's total center of gravity is calculated by adding the products of the components' overall masses with their distances from the reference line to their respective center of masses and dividing the resulting sum by the total mass of the rocket. In our rocket, the tip of the nose cone was chosen as the reference line. Rocket components that heavily contributed to the rocket's total mass were taken into consideration. This included the rocket's nose cone, body tube, the payload (control system), and the motor, as shown below:

$$CG_r = \frac{(CG_n + x_n)m_n + (CG_b + xb)m_b + (CG_p + x_p)m_p + (CG_m + x_m)m_m}{m_r}. \quad (4)$$

Both the tail fins and canard fins of the rocket were not taken into consideration, as their individual masses were very small compared to the total mass of the rocket.

The center of gravity for the rocket's nose cone was determined the same way as for a cylindrical cone, as shown by Equation 5:

$$CG_n = \frac{2l_n}{3}, \quad (5)$$

where l_n is the length of the nose cone.

A cone's center of gravity is normally located a third of its height from its base. So, since the rocket's reference line was made to be at the tip of the nose cone, two-thirds of the cone's height are considered instead.

The body tube and motor of a rocket are treated as uniform cylinders, while the rocket's payload is treated as a uniform rectangular. Both their respective centers of gravity were ultimately half of their total length, as shown in Equation 6:

$$CG_{b,p,m} = \frac{l_{b,p,m}}{2}. \quad (6)$$

Center of Pressure

In general, calculating the center of pressure requires determining the integral of pressure times the unit normal, multiplied by the area and the distance from the reference line, then divide by the integral of pressure multiplied by both the unit normal and area. Finding the center of pressure for a model rocket, however, can be simplified. Since the magnitude of pressure variation throughout the rocket is quite small, pressure can be treated as constant. In addition, model rockets are essentially symmetrical around their roll axis. These two assumptions reduce finding the center of pressure from a three-dimensional problem to a two-dimensional cut through the rocket's axis.

Thus, the center of pressure was determined from components of the rocket with surfaces exposed to air, specifically the nose cone, the body tube, and the tail and canard fins. Similarly to the rocket's total center of gravity, its total center of pressure is the sum of products of the components' distances from the tip of the nose cone to their centers and their planform area—their two-dimensional projected area—divided by the total planform area of the rocket:

$$CP_r = \frac{d_n A_n + d_b A_b + d_{tf} A_{tf} + d_{cf} A_{cf}}{A_r}. \quad (7)$$

The following equations were used in determining the planform area of the various components:

Nose Cone (triangle):

$$A_c = \frac{1}{2} d_c h_c, \quad (8)$$

where d_c and h_c are the nose cone's diameter and height.

Body Tube (rectangle):

$$A_b = d_b h_b, \quad (9)$$

where d_b and h_b are the body tube's diameter and height.

Tail Fins and Canard Fins (trapezoid):

$$A_{tf,cf} = \frac{1}{2} l_s (l_r + l_t), \quad (10)$$

where l_s is the fin span, l_r is the root chord length of the fin, and l_t is the tip chord length of the fin.

Results

From these calculations, the rocket's total center of mass was located 102 cm from the tip of the nose cone, while its total center of pressure was located 116 cm from the nose cone tip. With a rocket diameter of 10.4 cm, these results yielded a static stability of 1.34 body calibers, which met the intended stability margin of 1.0 and 2.0 body calibers and satisfied both our initial design parameters and the competition guidelines initially stated in the report.

7.2 Dynamic Stability

The dynamic response of a system can be used to analyze how a system behaves under a particular dynamic force. For our rocket, determining its dynamic stability gave us a better understanding of how our rocket behaves after experiencing an external disturbance(s) during flight. In addition, it helped us determine whether or not it would continue to oscillate during flight and develop a design based on that behavior.

Damping Ratio

The damping ratio of a dynamic response is a dimensionless number that describes how oscillations decay in a system. In the case where our rocket is the dynamic system analyzed, we defined the damping ratio in Equation 11:

$$\zeta = \frac{C_2}{2\sqrt{C_1 I_L}}, \quad (11)$$

where I_L is the longitudinal moment of inertia of the rocket, C_1 is the corrective moment coefficient of the rocket (Equation 12), and C_2 is the damping moment coefficient of the rocket (Equation 13), which is comprised of both the radial and axial damping moment coefficient, as shown in Equations 14 and 15.

$$C_1 = \frac{1}{2} \rho V^2 A_{r,fin} C_N (CP_r - CG_r), \quad (12)$$

$$C_2 = C_{2,A} + C_{2,R}, \quad (13)$$

$$C_{2,A} = \frac{1}{2} \rho V^2 A_{r,fin} [C_{N,fin}(Z_{fin} - CG_r)^2 + C_{N,cone}(Z_{cone} - CG_r)^2], \quad (14)$$

$$C_{2,R} = \dot{m}(Z_{cone} - CG_r)^2. \quad (15)$$

From Equations 12, 14, and 15, ρ and V are the fluid density and velocity of air while the rocket is in flight, and CG_r and CP_r are the rocket's total center of gravity and center of pressure. A_r is the reference area and Z is the distance from the tip of the nose cone to the leading edge for both the fin and nose cone. Finally, \dot{m} represents the change in mass of the rocket due to consumption of the propellant.

Originally, when considering the initial design of the rocket, we aimed for a critical damping ratio where $\zeta = 1$, because would minimize oscillations that our rocket would experience to one and in the system, and the rocket would return to equilibrium in the minimum amount of time. This type of response is, indeed, ideal for a rocket experiencing a single, significant disturbance. However, a rocket is more likely to experience continuous, small disturbances in flight, and with a critical damping ratio, the rocket will be susceptible to weathercocking. Instead, we found it was better to opt for an underdamped damping ratio, in which $\zeta < 1$; by allowing the rocket to oscillate, weathercocking will be minimized.

Since our rocket's velocity is changing with time, and the damping ratio is a function of velocity, we are given a range. Thus, we found the resulting damping ratio to be between 0.82 and 0.89 ($0.82 \leq \zeta \leq 0.89$) giving us an underdamped dynamic response.

Homogeneous Response

A homogeneous response was first analyzed to see how our rocket would behave in an ideal flight where there are no disturbances. The general second-order differential equation of this system is shown below in Equation 16.

$$I_L \frac{d^2 \alpha_x}{dt^2} + C_2 \frac{d\alpha_x}{dt} + C_1 \alpha_x = 0, \quad (16)$$

α_x is the rotational speed (angular velocity) of the rocket with respect to the yaw axis in rad/s.

Solving this differential equation gives the following general solution:

$$\alpha_x = Ae^{-Dt} \sin(\omega t + \phi), \quad (17)$$

where D is the inverse time constant, and ω is the natural frequency, both defined in Equations 18 and 19 below:

$$D = \frac{C_2}{2I_L}, \quad (18)$$

$$\omega = \sqrt{\frac{C_1}{I_L}}. \quad (19)$$

The amplitude A and phase shift ϕ are constants to be determined by initial conditions. Since our rocket is stationary just before flight and starts at an initial position of 0, $A = 1$ and $\phi = 0$.

Step Response

A step response was then analyzed after a homogeneous response to see how our rocket would behave after experiencing a step disturbance after launch. The general second-order differential equation of this system is shown below in Equation 20 below.

$$I_L \frac{d^2 \alpha_x}{dt^2} + C_2 \frac{d\alpha_x}{dt} + C_1 \alpha_x = M_s. \quad (20)$$

The term M_s represents an arbitrary yawing moment with an arbitrary value of 0.222 N-m, acts as a step for the system. Solving this differential equation gives the following general solution shown in Equation 21.

$$\alpha_x = (A_1 + A_2 t) e^{-Dt} \sin(\omega t + \phi). \quad (21)$$

Both D and ω are defined the same way. Due the same previous initial conditions of the rocket, $A_1 = 0$, $A_2 = 1$, and $\phi = 0$.

Analysis of Results

Figure 10 and Figure 11 show plots for both the homogeneous response and step response of the rocket.

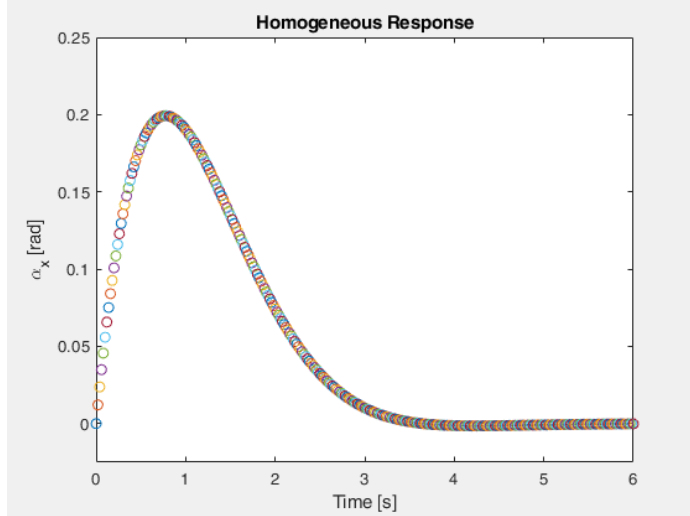


Figure 10: Underdamped homogeneous response of the rocket.

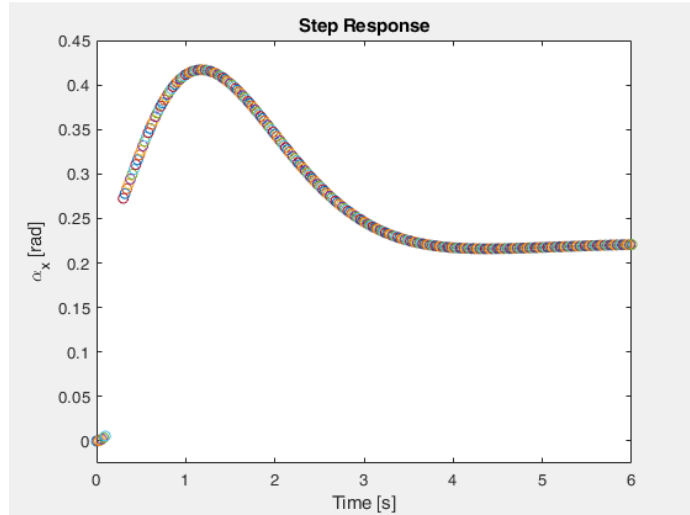


Figure 11: Underdamped step response of the rocket.

It is evident from the plots that, in both cases, the rocket experiences underdamping. However, since the range for the damping ratio is close to one, oscillations are still minimized and still resembles a critically damped response. A more ideal range for the damping ratio would be between 0.05 and 0.3.

7.3 Finite Element Analysis: Mode Shapes

Modal analysis was used to study the dynamic properties of the rocket in the frequency domain and determine its natural frequencies should it vibrate and experience resonance. For this project, the rocket was simulated as a six-degree-of-freedom rigid body—a solid body in which deformation is so small it could be neglected—as it acts as a three-dimensional body with no fixed ends or supports during flight.

A modal vibration is characterized by both a modal frequency and a mode shape. Normally, a mode shape is numbered according to the number of half waves in the vibration. However, since the rocket is a three-dimensional body with six degrees of freedom, the mode shape number corresponds to vibration in that translation / rotational axis, specifically the translational x, y, and z axes and the rotational roll, yaw, and pitch axes. Table 3 shows the first six mode shapes of the rocket and the corresponding natural frequencies. These modes and frequencies were obtained using a frequency analysis simulation of a mesh of our rocket's body in Solidworks, and the material properties used in calculating these results were the Young Modulus and density.

Table 3: Natural frequencies for the first six modes of the rocket.

Mode	Frequency (Hz)
1	0
2	7.05E-4
3	1.36E-4
4	2.78E-4
5	0.21
6	1.37

Being a six-degrees-of-freedom rigid body, the rocket should have natural frequencies equal to zero or very close to zero for the first six mode shapes. As shown in Table 3, Modes 1-4 have a natural frequency that is very close to 0 Hz. However, Mode 5 and Mode 6 instead have corresponding natural frequencies of 0.21 Hz and 1.31 Hz. The total deformation of Modes 5 and 6 are shown below in Figure 14 and Figure 15, with the resultant displacement scale bar shown

in Figure 16. It is important to note that the scale bar does show the actual displacement of the rocket, as the actual displacements depend on the input excitation, and the simulation inputs resonant frequencies, which theoretically gives infinite displacements.

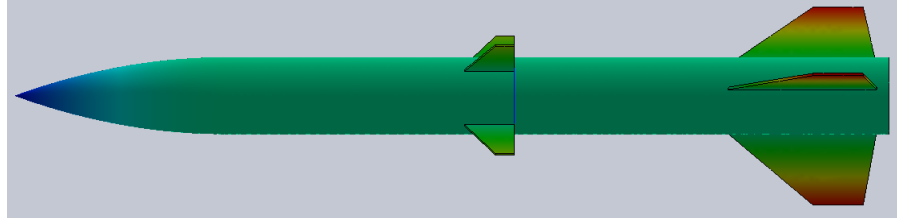
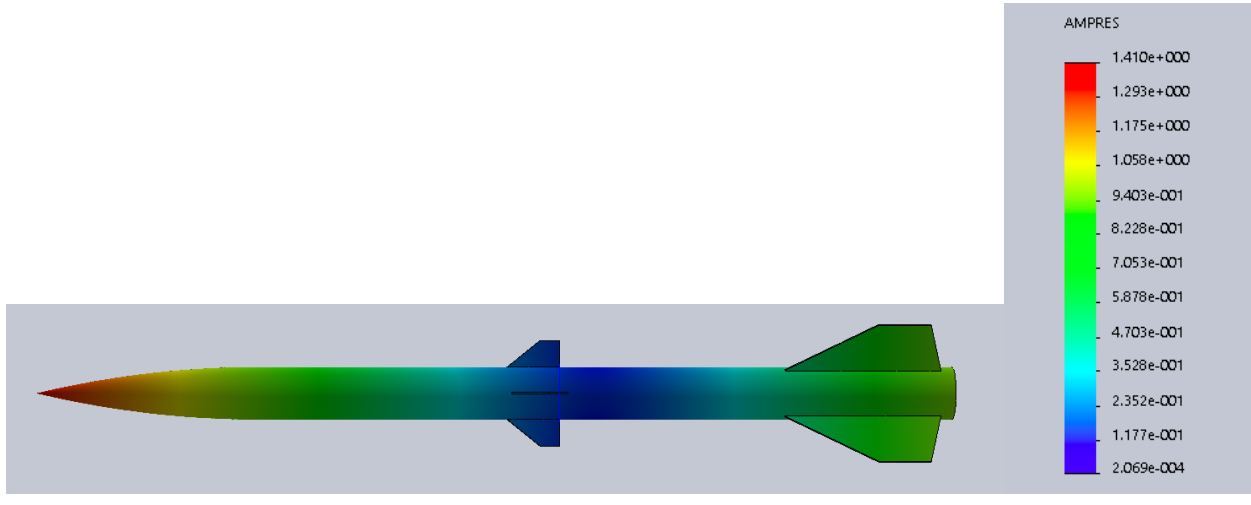


Figure 12: Deformation of the rocket at a 0.21 Hz resonant frequency of Mode 5.



(a) Deformation of the rocket at a 1.37 Hz resonant frequency of Mode 6.

(b) Scale bar.

Figure 13: Mode shape results.

It can be seen in comparing Mode 5 and Mode 6 that the displacement in Mode 5 shows the rocket body expanding across its body axis.

Because the natural frequencies of Mode 5 and Mode 6 are two and three orders of magnitude larger than the natural frequencies of the previous mode shapes, it was inferred that these two nonzero frequencies were the result of incompatible meshing in the modal analysis simulation of the rocket. Mode 5 and Mode 6 correspond to two of the three rotational axes of the rocket, and these two axes therefore have inconsistent meshing. It is difficult to conclude, nonetheless, which axes (roll, yaw, or pitch) have inconsistent meshing based on the deformation across the

body of the rocket shown in Figure 12 and Figure 13.

7.4 Drag Coefficient and Digital DATCOM

In order to theoretically determine the aerodynamic coefficients of the whole rocket assembly, the rocket was divided into three distinct sections: the top, which included the nose cone and concealed parachute; middle, which included the canard fins and upper half of the body tube; and bottom, which included the motor, tail fins, and lower half of the body tube. Calculations were done in Matlab for our initially chosen rocket dimensions, and they were modified until we achieved our desired stability margin.

Drag

The equations used for determining the coefficient of drag force on the rocket are obtained from the Mandell book for advanced rocketry. The main components of the rocket that contributed to the drag force are the body, base, tail fins, and canard fins. In addition, there is also drag induced by the interference effects between the body and fins.

Friction Force Coefficient:

In order to calculate the drag on the rocket due to viscous friction, the friction force coefficient must first be determined by the following equation:

$$C_f = \begin{cases} \frac{1.328}{\sqrt{Re}} & \text{when } Re \leq Re_c, \\ \frac{0.074}{Re^{1/5}} - \frac{B}{Re} & \text{when } Re \geq Re_c, \end{cases} \quad (22)$$

where B is given by this equation;

$$B = Re_c \left(\frac{0.074}{Re^{1/5}} - \frac{1.328}{\sqrt{Re}} \right), \quad (23)$$

and Re and Re_c are the Reynolds and critical Reynolds number, where the former is given by this equation:

$$Re = \frac{\rho V L}{\mu}, \quad (24)$$

with ρ , V , L , and μ being the density of the air, the apparent velocity vector, the characteristic dimension, and the dynamic viscosity of air.

Body Drag:

The drag on the rocket's body is calculated using the following equation:

$$C_{D(fb)} = \left[1 + \frac{60}{(l_{TR}/d_b)^3} + 0.0025 \frac{l_b}{d_b} \right] \left[2.7 \frac{l_n}{d_b} + 4 \frac{l_b}{d_b} \right] C_f, \quad (25)$$

where l_{TR} , l_b , and l_n are the length of total length of the rocket, the length of the body tube, and the length of the nose cone, and d_b and d_d are the diameters of the body tube and base of the rocket.

Base Drag:

The drag from the base of the rocket is given by the following equation:

$$C_{D(b)} = 0.029 \frac{\left(\frac{d_b}{d_d}\right)^3}{\sqrt{C_{D(fb)}}}. \quad (26)$$

Tail Fins / Canard Fins Drag:

Fin drag on the rocket at a zero attack angle is determined by the following equation:

$$C_{D(f)} = 2C_f \left(1 + \frac{T_f}{l_m} \right) \frac{4nA_{fp}}{\pi d_f^2}, \quad (27)$$

where T_f is the fin thickness, l_m is the true length of the fin from inner to outer edge, n is the number of fins, and A_{fp} is the fin planform area.

Interference Drag:

Finally, the drag due to interference effects between the body and fins of the rocket is determined by the following equation:

$$C_{D(f)} = 2C_f \left(1 + \frac{T_f}{l_m} \right) \frac{4n(A_{fp} - A_{fe})}{\pi d_f^2}, \quad (28)$$

where A_{fe} is the exposed part of the trapezoidal fin area.

Total Drag:

Thus, the total drag force coefficient of the rocket is the sum of each of the drag coefficients from each main rocket component:

$$C_D = C_{D(fb)} + C_{D(b)} + C_{D(d)} + CD(f). \quad (29)$$

Results:

The total drag force coefficient of the rocket was calculated to be 0.15 at a zero attack angle. This value matches up with the Open Rocket simulation, verifying our code.

Digital DATCOM

The rest of the aerodynamic coefficients – dynamic and control derivatives, to be more specific – were determined using Digital DATCOM. Such aerodynamic coefficients are a function of both Mach number and angle of attack; therefore, DATCOM determined the dynamic and control derivatives for different combination of Mach number and angle of attack to make the 6DOF model more accurate. Digital DATCOM is only for airplane configuration, which means that the rocket had to be treated as a body-wing configuration. Because of this, only two front canards could be included, while the other two were omitted. Due to ITAR regulations, which were mentioned earlier, results for the dynamic and control derivatives will not published on this paper.



Figure 14: DATCOM Model.

7.5 Computational Fluid Dynamics

With the use of Computational Fluid Dynamics, the team was able to gain a much deeper understanding of the fluid flow around the whole aerostructure. Gaining this knowledge was extremely important because analysis of the system's response and calculations of the aerodynamic coefficients was done with assumption of subsonic flow. Therefore, it was imperative to check that this assumption was correct in order to make sure the results acquired were correct. Figure x and y show the results of such fluid flow computation.

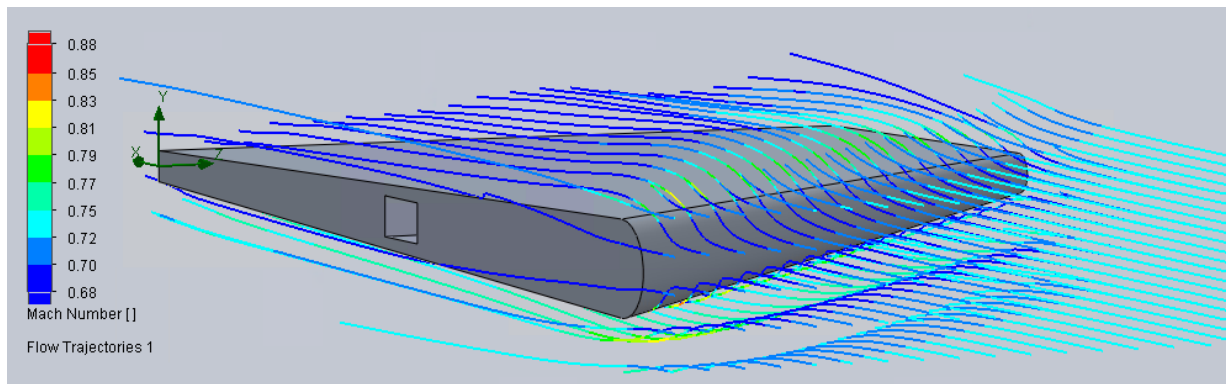


Figure 15: Fluid flow around one canard fin.

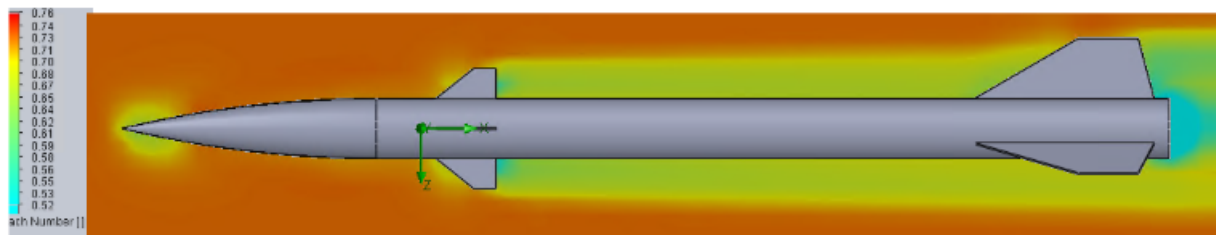


Figure 16: Fluid flow around the entire body at maximum velocity.

As can be seen from both Figure 15 and 16, the flow around the main body components stays within the subsonic region, validating the assumption made to conduct the analysis.

8 Flight Dynamics

To design the control system, a 6 degrees-of-freedom (6DOF) mathematical model of the flight dynamics was constructed in Matlab®Simulink. It is 6 degrees because of the three parameters needed to fully describe the translation motion (x,y,z), in addition to three more parameters needed to describe the rotational motion (p,q,r).

For the 6DOF simulation, the entire rocket assembly (minus control system) was analyzed. Such assembly includes the aerostructure, canard fins, rocket motor, and payload weight. The external environment that has been applied only includes the wind profile. This is sufficient for the external environment because flight dynamics are greatly affected by the wind than any other outside factors. The modeling approach for the flight trajectory of the rocket using 6DOF was Simulink. As for the assumptions made, there were many assumptions that were needed to be made in order to greatly simplify the modeling approach. Some of the most important assumptions made were that the angle of attack is small in magnitude (< 5 degrees), the Coriolis acceleration due to the earth's rotation is neglected, the thrust force only acts longitudinally, the aerostructure is a rigid body, and the inertial frame is a flat earth.

8.1 Six Degrees-of-Freedom (6DOF) Mathematical Model

Before proceeding to the equations of motion, all the reference frames that are used for the model must be introduced. As mentioned earlier, a flat earth frame is used as the inertial frame for the system. This frame is located at the launch pad, and it is denoted by the subscript, e ; i.e., no the inertial frame is denoted by (X_e, Y_e, Z_e) . The structure and body frame are attached to the rocket. The structure frame (i_s, j_s, k_s) has its origin at the tip of the nose cone, while the body frame (i, j, k) has its origins attached to the center of mass of the rocket. Refer to Figure 17 for a better understanding of the frames

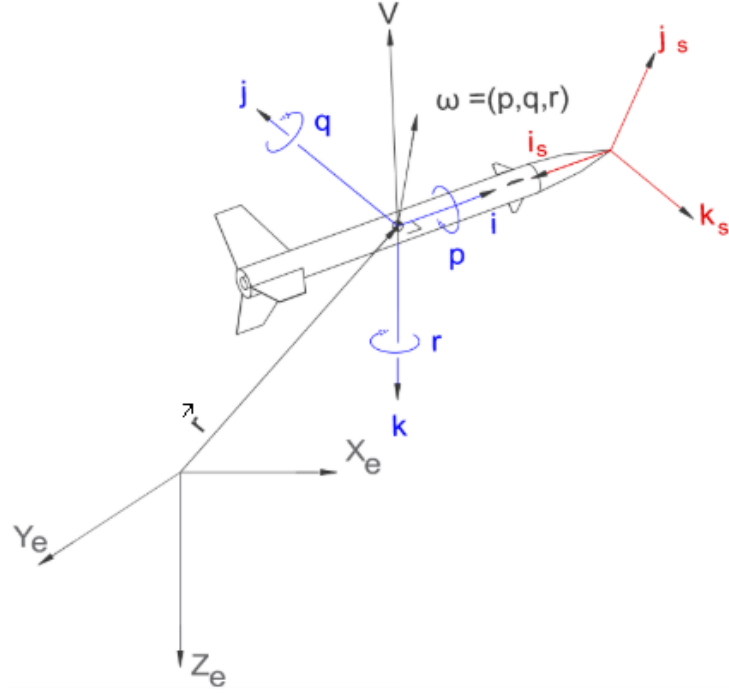


Figure 17: Inertial frame and its relationship to the structure frame and body frame.

Rotation Kinematics and Rotational Matrix

The rocket, soon after taking off, may experience outside disturbances such as wind. The wind, combined with asymmetries in the body, cause torques about the rocket's center of mass, which most often cause the rocket to experience angular motion. Not to mention the effects that a spinning earth has on this motion. Looking at Figure 18, the angular rate vectors are shown on the rocket in the body frame. It must be noted that the aerodynamic forces act about the center of pressure.

The Euler's rotational equation of motion of a rigid vehicle is given as follows;

$$\dot{\vec{H}} = \dot{\vec{T}}, \quad (30)$$

where $\dot{\vec{H}}$ is the angular momentum vector and $\dot{\vec{T}}$ is the total external torque applied to the center of gravity of the vehicle. Eq. 30 may also be written as

$$\vec{H} = \vec{J} \cdot \vec{\omega}, \quad (31)$$

where $\vec{\omega}$ is the angular velocity vector of the rocket ($\vec{\omega} = p \vec{i} + q \vec{j} + r \vec{k}$), and \vec{J} is vehicle's

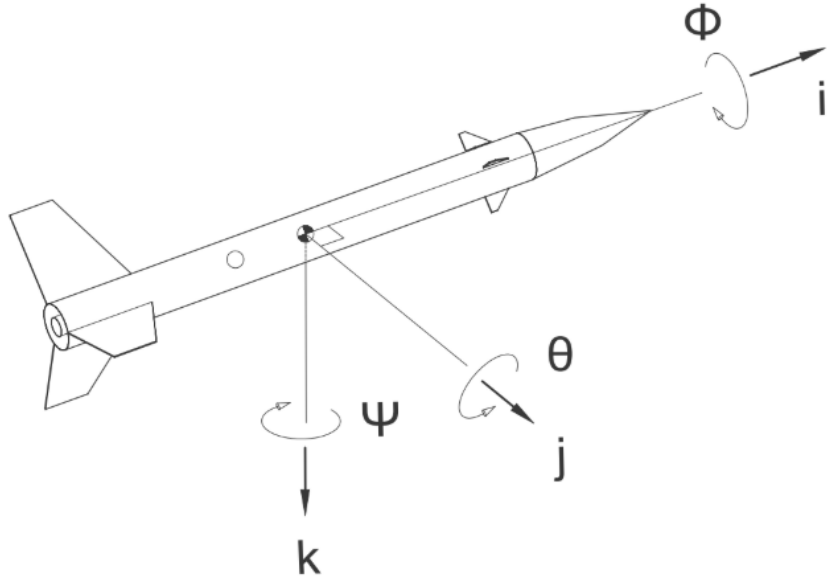


Figure 18: Body rates shown in the body frame.

inertia dyadic about the center of gravity and has the form:

$$\vec{J} = \begin{bmatrix} J_{xx} & J_{xy} & J_{xz} \\ J_{yx} & J_{yy} & J_{yz} \\ J_{zx} & J_{zy} & J_{zz} \end{bmatrix}. \quad (32)$$

With Eq. 32, the rotational equation of motion becomes:

$$\vec{J} \cdot \vec{\omega} + \vec{\omega} \times \vec{J} \cdot \vec{\omega} = \vec{M}_{aero}. \quad (33)$$

The rotational kinematic equation for the three Euler angles (ϕ, θ, ψ) is given by the following expression:

$$\begin{bmatrix} \dot{\phi} \\ \dot{\theta} \\ \dot{\psi} \end{bmatrix} = \frac{1}{\cos(\theta)} \begin{bmatrix} \cos(\theta) & \sin(\phi)\sin(\theta) & \cos(\phi)\sin(\theta) \\ 0 & \cos(\phi)\cos(\theta) & -\sin(\phi)\cos(\theta) \\ 0 & \sin(\phi) & \cos(\phi) \end{bmatrix} \begin{bmatrix} p \\ q \\ r \end{bmatrix}. \quad (34)$$

However, as can be noted from Eq.34, a singularity happens when $\theta = 90$ degrees. This singularity can be avoided by using quaternions; Eq. 34 in terms of quaternions (q_1, q_2, q_3, q_4)

is as follows:

$$\begin{bmatrix} \dot{q}_1 \\ \dot{q}_2 \\ \dot{q}_3 \\ \dot{q}_4 \end{bmatrix} = \frac{1}{2} \begin{bmatrix} 0 & r & -q & p \\ -r & 0 & p & q \\ q & -p & 0 & r \\ -p & -q & -r & 0 \end{bmatrix} \begin{bmatrix} q_1 \\ q_2 \\ q_3 \\ q_4 \end{bmatrix}, \quad (35)$$

which is subjected to the normalization constraint $q_1^2 + q_2^2 + q_3^2 + q_4^2 = 1$. The coordinate transformation matrix to the body frame from the inertial frame in terms of quaternions is given by the following expression:

$$C^{B/I} = \begin{bmatrix} 1 - 2(q_2^2 + q_3^2) & 2(q_1 q_2 + q_3 q_4) & 2(q_1 q_3 - q_2 q_4) \\ 2(q_1 q_2 - q_3 q_4) & 1 - 2(q_1^2 + q_3^2) & 2(q_2 q_3 + q_1 q_4) \\ 2(q_1 q_3 + q_2 q_4) & 2(q_2 q_3 - q_1 q_4) & 1 - 2(q_1^2 + q_2^2) \end{bmatrix}. \quad (36)$$

And to the inertial frame from the body frame we have:

$$\begin{aligned} C^{I/B} &= [C^{B/I}]^{-1} = [C^{B/I}]^T \\ &= \begin{bmatrix} 1 - 2(q_2^2 + q_3^2) & 2(q_1 q_2 - q_3 q_4) & 2(q_1 q_3 + q_2 q_4) \\ 2(q_1 q_2 + q_3 q_4) & 1 - 2(q_1^2 + q_3^2) & 2(q_2 q_3 - q_1 q_4) \\ 2(q_1 q_3 - q_2 q_4) & 2(q_2 q_3 + q_1 q_4) & 1 - 2(q_1^2 + q_2^2) \end{bmatrix}. \end{aligned} \quad (37)$$

Aerodynamic Forces and Moments

Right after launch, the rocket experiences forces due to gravity, the motor, and the fluid flow. These forces must be taken into account in order to formulate a precise model for the flight dynamics. Looking at Figure 19, the direction of each force can be better appreciated.

The aerodynamic forces are expressed in the body-axis frame as follows:

$$D = C_A Q S,$$

$$C = C_{Y_\beta} \beta Q S, \quad (38)$$

$$N = (C_{N_0} + C_{N_\alpha}) Q S,$$

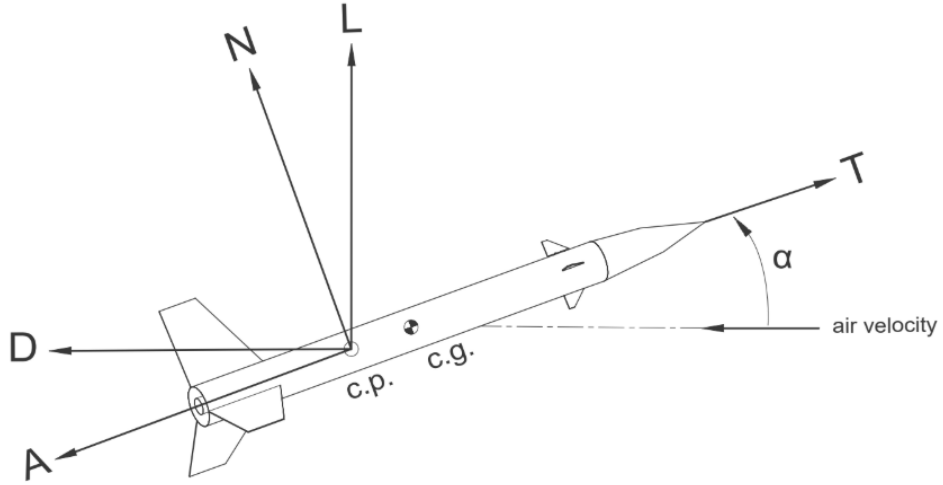


Figure 19: Forces acting on body shown in the body frame.

where Q is the dynamic pressure, α is the angle of attack, and β is the sideslip angle, which are defined as follows:

$$Q = \frac{1}{2} \rho V_m^2, \quad (39)$$

$$\alpha = \tan^{-1} \left(\frac{V_{m \cdot zb}}{V_{m \cdot xb}} \right), \quad (40)$$

$$\beta = \sin^{-1} \left(\frac{V_{m \cdot yb}}{V_m} \right), \quad (41)$$

where V_m is the body-axis vehicle's airstream velocity, ρ is the air density, which is a function of altitude. Moving on, we have:

$$F_{aero \cdot xb} = -D,$$

$$F_{aero \cdot yb} = C, \quad (42)$$

$$F_{aero \cdot zb} = -N.$$

As for the they aerodynamic moments about the center of gravity, they are expressed in the body-axis frame as follows:

$$\begin{bmatrix} M_{aero \cdot xb} \\ M_{aero \cdot yb} \\ M_{aero \cdot zb} \end{bmatrix} = \begin{bmatrix} C_{M_{r\beta}} Q S b \\ (C_{M_{p0}} + C_{M_{pa}} \alpha) Q S b \\ C_{M_{y\beta}} \beta Q S b \end{bmatrix}, \quad (43)$$

where S and b are the vehicle's reference area and length, respectively.

The gravity model for this project has been greatly reduced from the J_4 gravity model. The reduced model is as follows:

$$\begin{bmatrix} g_x \\ g_y \\ g_z \end{bmatrix} = -\frac{\mu}{r^2} \begin{bmatrix} X/r \\ Y/r \\ Z/r \end{bmatrix}, \quad (44)$$

where $r = \sqrt{X^2 + Y^2 + Z^2}$.

The body-axis components of the thrust force are

$$\begin{bmatrix} F_{thrust \cdot xb} \\ F_{thrust \cdot yb} \\ F_{thrust \cdot zb} \end{bmatrix} = \begin{bmatrix} T \\ 0 \\ 0 \end{bmatrix}. \quad (45)$$

Summary of the 6-DOF Equations of Motion

The total forces expressed in the body frame are:

$$\begin{bmatrix} F_{total \cdot xb} \\ F_{total \cdot yb} \\ F_{total \cdot zb} \end{bmatrix} = \begin{bmatrix} F_{aero \cdot xb} \\ F_{aero \cdot yb} \\ F_{aero \cdot zb} \end{bmatrix} + \begin{bmatrix} F_{thrust \cdot xb} \\ F_{thrust \cdot yb} \\ F_{thrust \cdot zb} \end{bmatrix} + C^{B/I} \begin{bmatrix} F_{w \cdot xb} \\ F_{w \cdot yb} \\ F_{w \cdot zb} \end{bmatrix} \quad (46)$$

$$= \begin{bmatrix} C_A Q S \\ C_{Y\beta} \beta Q S \\ (C_{N_0} + C_{N\alpha}) Q S \end{bmatrix} + \begin{bmatrix} T \\ 0 \\ 0 \end{bmatrix} + C^{B/I} \begin{bmatrix} mg \\ mg \\ mg \end{bmatrix}. \quad (47)$$

The total forces expressed in the inertial frame are:

$$\begin{bmatrix} F_{total \cdot xi} \\ F_{total \cdot yi} \\ F_{total \cdot zi} \end{bmatrix} = C^{I/B} \begin{bmatrix} F_{total \cdot xb} \\ F_{total \cdot yb} \\ F_{total \cdot zb} \end{bmatrix}. \quad (48)$$

The translational equations of motion in the inertial frame are:

$$\begin{bmatrix} \ddot{X} \\ \ddot{Y} \\ \ddot{Z} \end{bmatrix} = \frac{1}{m} \begin{bmatrix} F_{total \cdot xi} \\ F_{total \cdot yi} \\ F_{total \cdot zi} \end{bmatrix}. \quad (49)$$

The rotational equations of motion in the inertial frame are:

$$\begin{bmatrix} J_{xx} & J_{xy} & J_{xz} \\ J_{yx} & J_{yy} & J_{yz} \\ J_{zx} & J_{zy} & J_{zz} \end{bmatrix} \begin{bmatrix} \dot{p} \\ \dot{q} \\ \dot{r} \end{bmatrix} = - \begin{bmatrix} 0 & -r & q \\ r & 0 & -p \\ -q & p & 0 \end{bmatrix} \begin{bmatrix} J_{xx} & J_{xy} & J_{xz} \\ J_{yx} & J_{yy} & J_{yz} \\ J_{zx} & J_{zy} & J_{zz} \end{bmatrix} \begin{bmatrix} p \\ q \\ r \end{bmatrix} + \begin{bmatrix} M_{aero \cdot xb} \\ M_{aero \cdot yb} \\ M_{aero \cdot zb} \end{bmatrix}, \quad (50)$$

$$\begin{bmatrix} \dot{q}_0 \\ \dot{q}_1 \\ \dot{q}_2 \\ \dot{q}_3 \end{bmatrix} = \frac{1}{2} \begin{bmatrix} 0 & -p & -q & -r \\ p & 0 & r & -q \\ q & -r & 0 & p \\ r & q & -p & 0 \end{bmatrix} \begin{bmatrix} q_0 \\ q_1 \\ q_2 \\ q_3 \end{bmatrix}. \quad (51)$$

8.2 Simulation Results

Looking at Figure 20, the maximum altitude (red line) achieved by the rocket is 3,065 m, which is just above our intended target altitude. As for the angular ratesm Figure 21 shows that the maximum pitching rate (green line) shows an oscillatory behavior throughout the ascent, which is in accordance to the results found from the dynamic stability analysis done in Section 5.2.

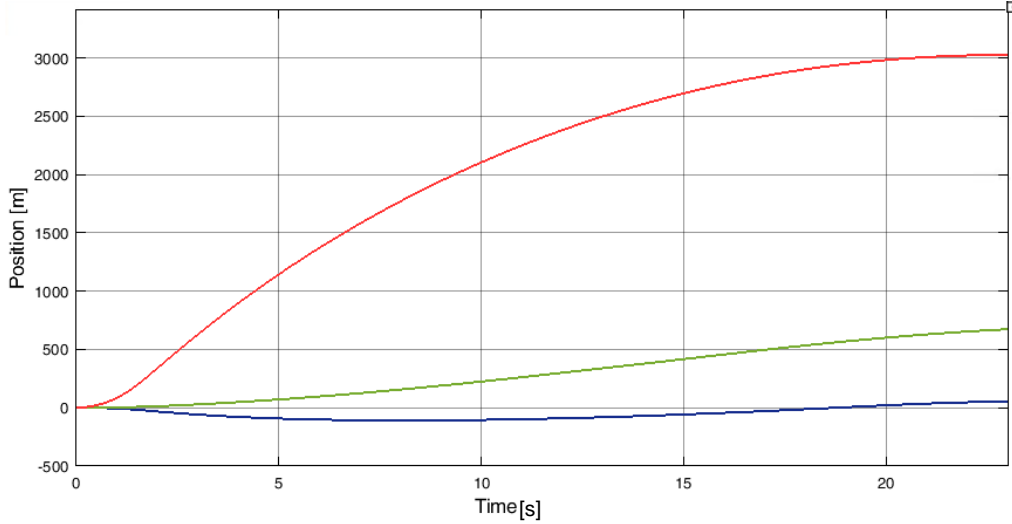


Figure 20: Altitude versus time acquired by the 6DOF simulation.

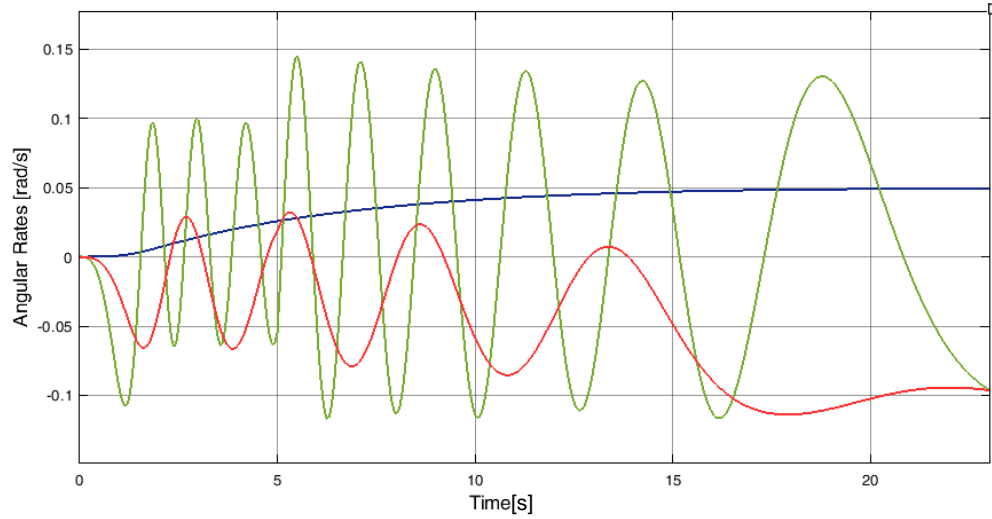


Figure 21: Angular rates versus time acquired by the 6DOF simulation.

8.3 Control System Design Via LQR

After verifying that the simulation results were correct, the model was linearized using Simulink's Control Design feature. Such linearized was done at 4 seconds in order to get the state-space representation of the system. Then the A,B,C,D matrices of the system were imported to Matlab® workspace, where the feedback gain matrix, \mathbf{K} , was determined using LQR (Linear Quadratic Regulator). The reason why LQR was implemented in designing the control system is because the model represented a multiple-input-multiple-output (MIMO) system, therefore the conventional form of loopshaping in scalar systems (SISO) could not be applied in this case.

What LQR does is it provides the optimal feedback gains to make an unstable system stable. To acquire this gain matrix, the plant must be written in state-space form $\dot{x} = Ax + Bu$, and that *all* of the number of states x of the system are available for the controller. Once the feedback gain matrix, \mathbf{K} , is determined, it is implemented as $u = -\mathbf{K}(x - x_d)$. With this, the system's dynamics are then expressed as:

$$\dot{x} = (A - BK)x + BKx_d, \quad (52)$$

where x_d represents the vector of desired states, and is the input to the closed-loop system. As seen from Eq. 39, the closed-loop system "A-matrix" becomes $(A-BK)x$, while the "B-matrix" becomes BKx_d . The linearized representation of the system is shown in the following two pages. When linearizing the model, every state was given a variable. For example, X, Y , and Z where given the variables Z_1 , Z_2 , and Z_3 , respectively.

Now this specific approach did not work because the team tried to force all the states to zero, when in fact the velocity and altitude components needed to change with time. This realization came late in the design stage, and so the necessary changes could not be made due to time constraints.

$$\begin{aligned}
f = & \frac{\mu Z_1}{(Z_1^2 + Z_2^2 + Z_3^2)^{3/2}} - \frac{CA0SQ(t)(1-2(Z_{11}^2 + Z_{12}^2))}{m(t)} + \frac{Fbase(1-2(Z_{11}^2 + Z_{12}^2))}{m(t)} + \frac{T(1-2(Z_{11}^2 + Z_{12}^2))}{m(t)} - \frac{2CN0SQ(t)(Z_{10}Z_{12} + Z_{11}Z_{13})}{m(t)} - \frac{2CN\alpha Stan^{-1}(Z_4, Z_6)Q(t)(Z_{10}Z_{12} + Z_{11}Z_{13})}{m(t)} + \frac{2CY\beta Ssin^{-1}\left(\frac{Z_5}{\sqrt{Z_4^2 + Z_5^2 + Z_6^2}}\right)Q(t)(Z_{10}Z_{11} - Z_{12}Z_{13})}{m(t)} \\
& \frac{\mu Z_2}{(Z_1^2 + Z_2^2 + Z_3^2)^{3/2}} + \frac{CY\beta Ssin^{-1}\left(\frac{Z_5}{\sqrt{Z_4^2 + Z_5^2 + Z_6^2}}\right)Q(t)(1-2(Z_{10}^2 + Z_{12}^2))}{m(t)} - \frac{2CN0SQ(t)(Z_{11}Z_{12} - Z_{10}Z_{13})}{m(t)} - \frac{2CN\alpha Stan^{-1}(Z_4, Z_6)Q(t)(Z_{11}Z_{12} - Z_{10}Z_{13})}{m(t)} - \frac{2CA0SQ(t)(Z_{10}Z_{11} + Z_{12}Z_{13})}{m(t)} + \frac{2Fbase(Z_{10}Z_{11} + Z_{12}Z_{13})}{m(t)} + \frac{2T(Z_{10}Z_{11} + Z_{12}Z_{13})}{m(t)} \\
& \frac{\mu Z_3}{(Z_1^2 + Z_2^2 + Z_3^2)^{3/2}} - \frac{CN0SQ(t)(1-2(Z_{10}^2 + Z_{11}^2))}{m(t)} - \frac{CN\alpha Stan^{-1}(Z_4, Z_6)Q(t)(1-2(Z_{10}^2 + Z_{11}^2))}{m(t)} + \frac{2CY\beta Ssin^{-1}\left(\frac{Z_3}{\sqrt{Z_4^2 + Z_5^2 + Z_6^2}}\right)Q(t)(Z_{11}Z_{12} + Z_{10}Z_{13})}{m(t)} - \frac{2CA0SQ(t)(Z_{10}Z_{12} - Z_{11}Z_{13})}{m(t)} + \frac{2Fbase(Z_{10}Z_{12} - Z_{11}Z_{13})}{m(t)} + \frac{2T(Z_{10}Z_{12} - Z_{11}Z_{13})}{m(t)} \\
& \frac{bCMr\beta SQ(t) + CN0cySQ(t) + CY\beta czSsin^{-1}\left(\frac{Z_5}{\sqrt{Z_4^2 + Z_5^2 + Z_6^2}}\right)Q(t) + CN\alpha cyS\alpha(t)Q(t) + JyZ_8Z_9 - JzZ_8Z_9}{Jx} \\
& \frac{-czFbase - czT + bCMp0SQ(t) + CA0czSQ(t) - CN0S(cx - Xa)Q(t) - CN\alpha S(cx - Xa)\tan^{-1}(Z_4, Z_6)Q(t) - JxZ_7Z_9 + JzZ_7Z_9 + bCMp\alpha SQ(t)\alpha(t)}{Jy} \\
& \frac{cyFbase + cyT - CA0cySQ(t) + CY\beta S(Xa - cx)\sin^{-1}\left(\frac{Z_5}{\sqrt{Z_4^2 + Z_5^2 + Z_6^2}}\right)Q(t) + JxZ_7Z_8 - JyZ_7Z_8 + bCM\beta SQ(t)\beta(t)}{Jz} \\
& \frac{1}{2}(Z_9Z_{11} - Z_8Z_{12} + Z_7Z_{13}) \\
& \frac{1}{2}(-Z_9Z_{10} + Z_7Z_{12} + Z_8Z_{13}) \\
& \frac{1}{2}(Z_8Z_{10} - Z_7Z_{11} + Z_9Z_{13}) \\
& \frac{1}{2}(-Z_7Z_{10} - Z_8Z_{11} - Z_9Z_{12})
\end{aligned}$$

$$g = \begin{vmatrix} 0 & 0 & 0 \\ 0 & 0 & 0 \\ 0 & 0 & 0 \\ -\frac{CA\delta SQ(t)(1-2(Z_{11}^2+Z_{12}^2))}{m(t)} - \frac{2CN\delta SQ(t)(Z_{10}Z_{12}+Z_{11}Z_{13})}{m(t)} & -\frac{CA\delta SQ(t)(1-2(Z_{11}^2+Z_{12}^2))}{m(t)} \\ -\frac{2CN\delta SQ(t)(Z_{11}Z_{12}-Z_{10}Z_{13})}{m(t)} - \frac{2CA\delta SQ(t)(Z_{10}Z_{11}+Z_{12}Z_{13})}{m(t)} & -\frac{2CA\delta SQ(t)(Z_{10}Z_{11}+Z_{12}Z_{13})}{m(t)} \\ -\frac{CN\delta SQ(t)(1-2(Z_{10}^2+Z_{11}^2))}{m(t)} - \frac{2CA\delta SQ(t)(Z_{10}Z_{12}-Z_{11}Z_{13})}{m(t)} & -\frac{2CA\delta SQ(t)(Z_{10}Z_{12}-Z_{11}Z_{13})}{m(t)} \\ \frac{CN\delta cySQ(t)}{Jx} & 0 \\ \frac{bCMp\delta SQ(t)+CA\delta czSQ(t)-CN\delta S(cx-Xa)Q(t)}{Jy} & \frac{CA\delta czSQ(t)}{Jy} \\ \frac{bCMp\delta SQ(t)+CA\delta czSQ(t)-CN\delta S(cx-Xa)Q(t)}{Jy} & \frac{CA\delta czSQ(t)}{Jy} \\ \frac{bCMy\delta SQ(t)-CA\delta cySQ(t)}{Jz} & -\frac{CA\delta cySQ(t)}{Jz} \\ 0 & 0 \\ 0 & 0 \\ 0 & 0 \end{vmatrix}$$

9 Electronics Bay Design

9.1 Previous Projects

Adriano Arcadipane's Masters Thesis in Aerospace Engineering was used as a reference in the development of the payload. Arcadipane's design included 1 servo to control rolling motion of the rocket body as shown in Figure 22. Other items shown are a GPS module, a printed circuit board, gyroscope, telemetry which form a base for the development of this project's payload.

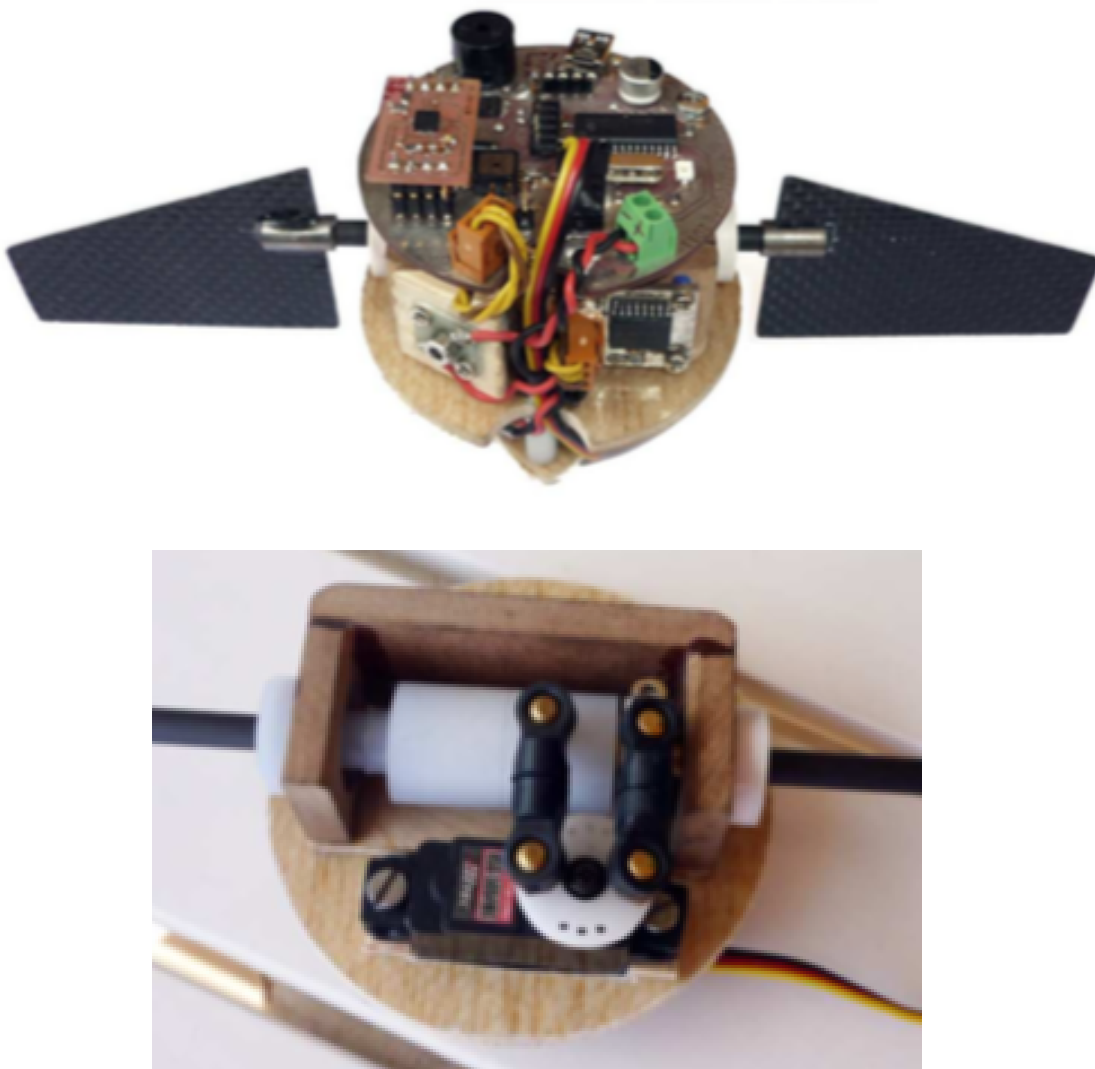


Figure 22: Adriano Arcadipane's payload design

The further scope of this project also intends to control yaw and pitch axis; therefore, a number of 4 servos are used to control each movement individually. The conceptual design

idea was based on Arcadipane's design to have a base understanding. Further improvements are intended to conform the final product.

9.2 Conceptual Design

The purpose of the electronics bay is to steer canard fins with actuators based on the Inertial Measuring Units (IMU) attitude values. The mathematical model will feed inputs into the controller to calculate the error based on attitude position at any given time. This error will be compensated by the actuators to maintain the desired rocket orientation. In addition, the electronics bay will house a barometric sensor and a logging system to record the altitude, angular speeds, and time of the flight. A GPS module and telemetry system will communicate location of the vehicle to retrieve the system once the rocket has landed.

A preliminary rendering of the system shown in Figure 23 indicates the concept of having actuators controlling fins; however, further research improved the design as many factors were later determined. Servo torque limits, power consumption, clockspeed, space and weight limitations amongst other constraints contributed to a more detailed design of the payload.

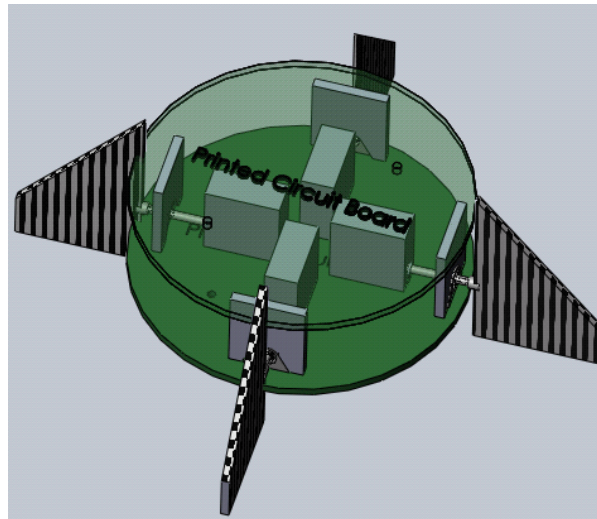


Figure 23: Rendering of preliminary concept design

A first prototype was developed using a Microcontroller Arduino Nano, 4x micro servos 9g and a IMU sensor MPU6050 from Adafruit. The code used was adapted from a 2DOF planar stabilization system using 2 micro servos 9g. In this code, the angular axis and calibration off-

set values of the IMU were determined for the purpose of this project as the IMU is oriented vertically as shown in Figure 24.

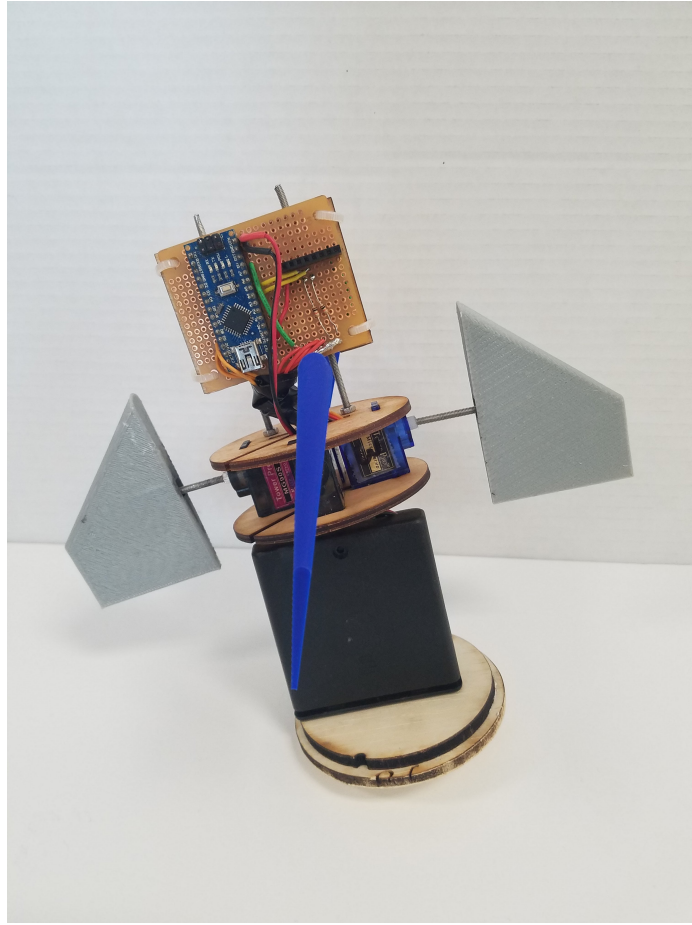


Figure 24: First payload prototype

9.2.1 Servo Motors

The chosen servo motor is Hitec Model Helicopter tailrotor HS5084-MG due to its speed of 0.07 seconds per 60 degrees. In order to model these actuators, a transfer function was determined according to its speed specifications of the form

$$G(s) = \frac{1}{1 + \tau s}, \quad (53)$$

In the response of a unit step shown in Figure 25, the time constant τ is determined by the point at which 63% of the time is presented.

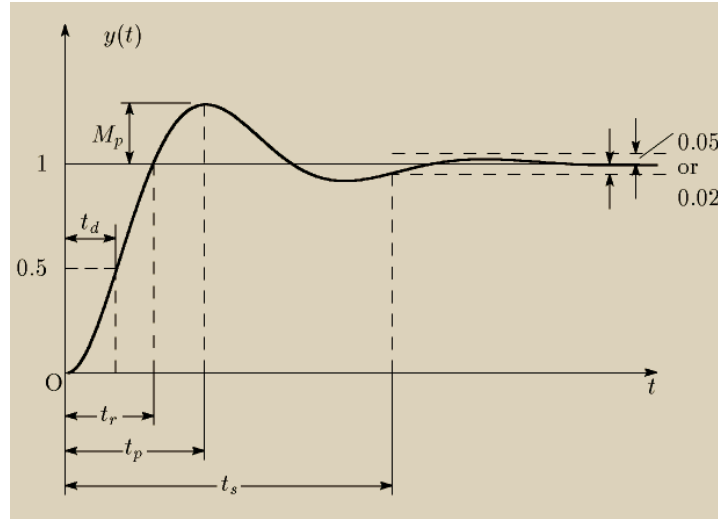


Figure 25: Plot of generic first order response under a unit step input. Figure depicted by Valeria Avila.

Where (td) is Delay time which is the time required for the response to reach half the final value the very first time. Rise time (tr) is the time required for the response to rise from 10% to 90%, 5% to 95%, or 0% to 100% of its final value. For underdamped second-order systems, the 0% to 100% rise time is normally used. For overdamped systems, the 10% to 90% rise time is commonly used. Peak time (tp) is the time required for the response to reach the first peak of the overshoot. Maximum (percent) overshoot (Mp) is the maximum peak value of the response curve measured from unity. Finally, settling time (ts) is the time required for the response curve to reach and stay within a range about the final value of size specified by absolute percentage of the final value (usually 2% or 5%). The settling time is related to the largest time constant of the control system.

In this case, 5% settling time is considered to find τ which corresponds to

$$t = 3\tau, \quad (54)$$

where t corresponds to time, and τ to time constant as defined previously.

If t is substituted by the specification of the servo motor to be 0.07 secs, then a time constant τ equals 0.0233. Therefore, the transfer function that models the servo motor is

$$G(s) = \frac{1}{1 + 0.0233s}, \quad (55)$$

9.2.2 Altimeter Data Logging

The payload will include a commercial off-the-shelf altimeter to log the peak altitude reached. Deciding factors on the altimeter architecture depend on commercial availability. The conceptual design includes an altimeter and data logging capabilities; however, further testing and research is required to decide when and how data is recorded. Options include in flight altitude logging using telemetry for live analysis from ground control. However, this comes with its own difficulties that must be addressed in the detailed design.

9.3 Prototype

Once the geometry from the preliminary design in Section 4 was defined, a prototype was developed using the open source platform Arduino nano board and the gyroscope and accelerometer IMU MPU6050 from Adafruit industries. The convenience of open source platform allowed for testing of simplified models to conceptualize the project. Figure 26 shows a prototype developed to test a simplified control system that corrected pitch and yaw.

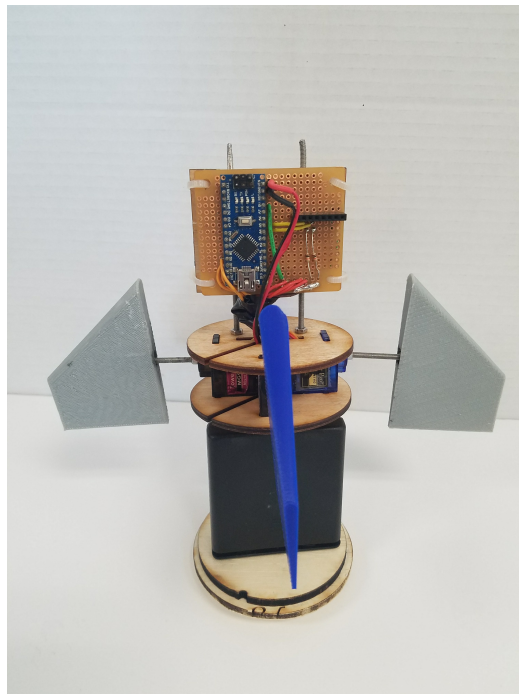


Figure 26: First control system prototype using Arduino and MPU6050 gyroscope.

The code used in this first prototype is based on a planar stabilization platform program

to maintain 2 axis (pitch and yaw) from disturbing a platform from its horizontal state. This program was then adapted to maintain canard fins vertical regardless of the rocket body tube's orientation. The sample code is shown in Appendix C.

The Arduino nano is connected to the servo motors and gyroscope as shown in Figure 27. A problem encountered with this initial design is that the nano was powering the servos and the sensor; however, the current draw from the four micro servos was so high that the batteries will drop voltage within minutes of continued use. Therefore, the next iteration shall have an independent power source for the servo motors as described in the schematic. This prototype is only using Microservos which tend to be less power consuming than higher torque servos; therefore, this improvement is imperative since the system must be on for at least half hour without interruption for data logging in launch.

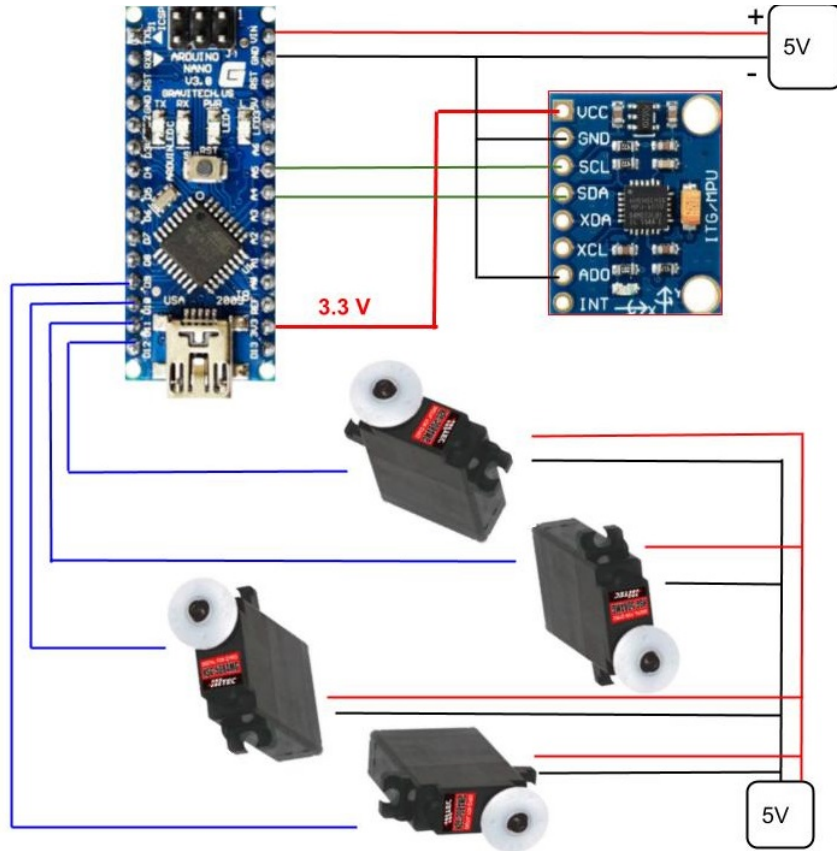


Figure 27: Schematic of the connections between the components of the circuit

This prototype served as a reference to the potential designs to keep the electronics stable, specifically the gyroscope to avoid vibrations disturbing the data recorded.

Lastly, design variations went into the connection between the canard fins and the servo motors. The shaft had to be designed to withstand the predicted aerodynamic forces presented during flight on the control surfaces. The final design required a thicker fin profile to enclose a shaft with enough clearance to avoid failure.

Once the geometry was finalized based on stability and other design requirements, the latest iteration of the payload was developed. Figure 28 shows the latest payload iteration that includes the same components as the prototype with improvements such as using rubber grommets to damp the vibrations caused by the flight on the electronics. This electronics bay is enclosed with a fiber glass coupler that connects two of the body tube components of the purchased kit. The fins were 3d printed and mounted as shown in Figure 28.

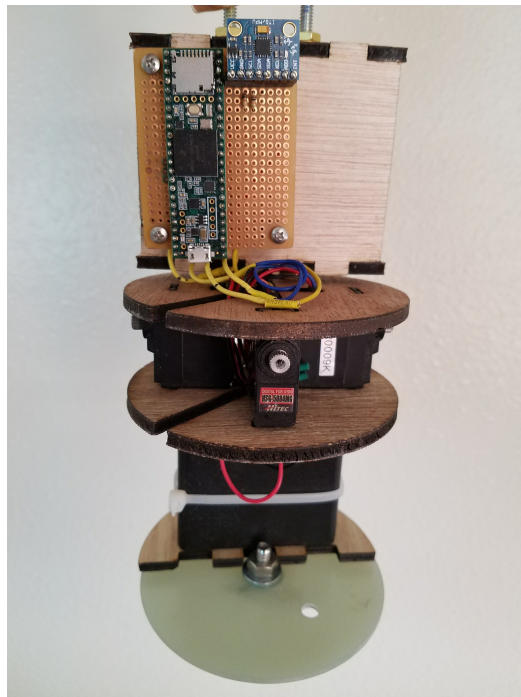


Figure 28: Latest iteration of the payload without canards installed.

Next steps with the payload is testing by simulating a flight and measuring the response and strength of the fins-shaft setup. In addition, the electronics will be acquiring altimeters and data logging capabilities to allow for in flight logging.



Figure 29: Payload enclosed with fiberglass coupler

10 Summary and Conclusions

The analysis shows that our rocket design is both statically and dynamically stable. In addition, every flight simulation shows that with our rocket configuration, our altitude goal of 3,000 [m] is achieved. Although the project was not completed, the team feels confident that once the control system is downloaded to the micro-controller, the system will behave in a similar manner as the analysis predicts. In addition, it must be kept in mind that this project is the first of its kind at SCU, and so not a lot of sources were available. With that being said, the team strongly believes that future teams will be much more successful because they will have a solid foundation available to them.

References

- [1] Rosanova, G. 2018, "Sounding Rockets Program Office" from
<https://www.wff.nasa.gov/code810/vehicles.html>
- [2] Mandell, G. K., 1973, *Topics in Advanced Model Rocketry*. MIT Press, Massachusetts.
- [3] Du, W., 2010, "Dynamic modeling and ascent flight control of Ares-I Crew Launch Vehicle", Ph.D. Thesis, Aerospace Engineering Department, Iowa State University.
- [4] Sampo N., 2010, "Development of an Open Source model rocket simulation software" M.S. thesis, Engineering Physics and Mathematics, Helsinki University Of Technology.
- [5] Barrowman J., 1967, "The Practical Calculation of the Aerodynamic Characteristics of Slender Finned Vehicles," M.S. thesis, Aerospace Engineering, The Catholic University of America.
- [6] Flynn G., 1969, "Model Rocketry: A Journal of Miniature Astronautics," *Model Rocketry*, 1(6), pp. 1-20.
- [7] Barrowman, J., 1966, "Fin: A Computer for Calculating the Aerodynamic Characteristics of Fins at Supersonic Speeds", NASA-TM-X-55523, Goddard Space Flight Center, Maryland.
- [8] Barrowman, J. 2012, "Calculating the Center of Pressure of a Model Rocket" , TR-33, Estes-Cox Corp.

11 Appendices

11.1 Appendix A: Market Research Findings

Customer:	Paul Reed	Interviewer:	Valeria Avila
Affiliation:	Tulsa Rocketry	Date:	10/23/17
Contact Info:	trprefect@gmail.com	Type of User:	Hobbyist, Educator
Question/Prompt	Customer Statement	Interpreted Need	
Applications of an active stabilization system?	The rocket going straight up because they are doing multi-stage projects or they want no roll because they have a camera on board.	Rocket flies vertically	
		No roll to allow for video and photographs	
Type of Payload required?	Any system that you would come up with would need to fit within the existing air frame sizes commonly used in high power rocketry	Payload fits within commonly used sizes in high power rocketry	
	It needs to be light because weight means lost altitude which is important to many hobbyists.	Payload is light and does not add significant weight to system	
Type of stabilization (roll, yaw, pitch)	Many combine a camera and would love to get a near-vertical-flight with no roll.	Rocket has no roll and flies vertically	
Accuracy	Multi stage projects all have a requirement that they stay within a tight band of vertical (< 5 degrees) for safety reasons.	Rocket's stabilization stays within < 5 degrees from vertical axis	

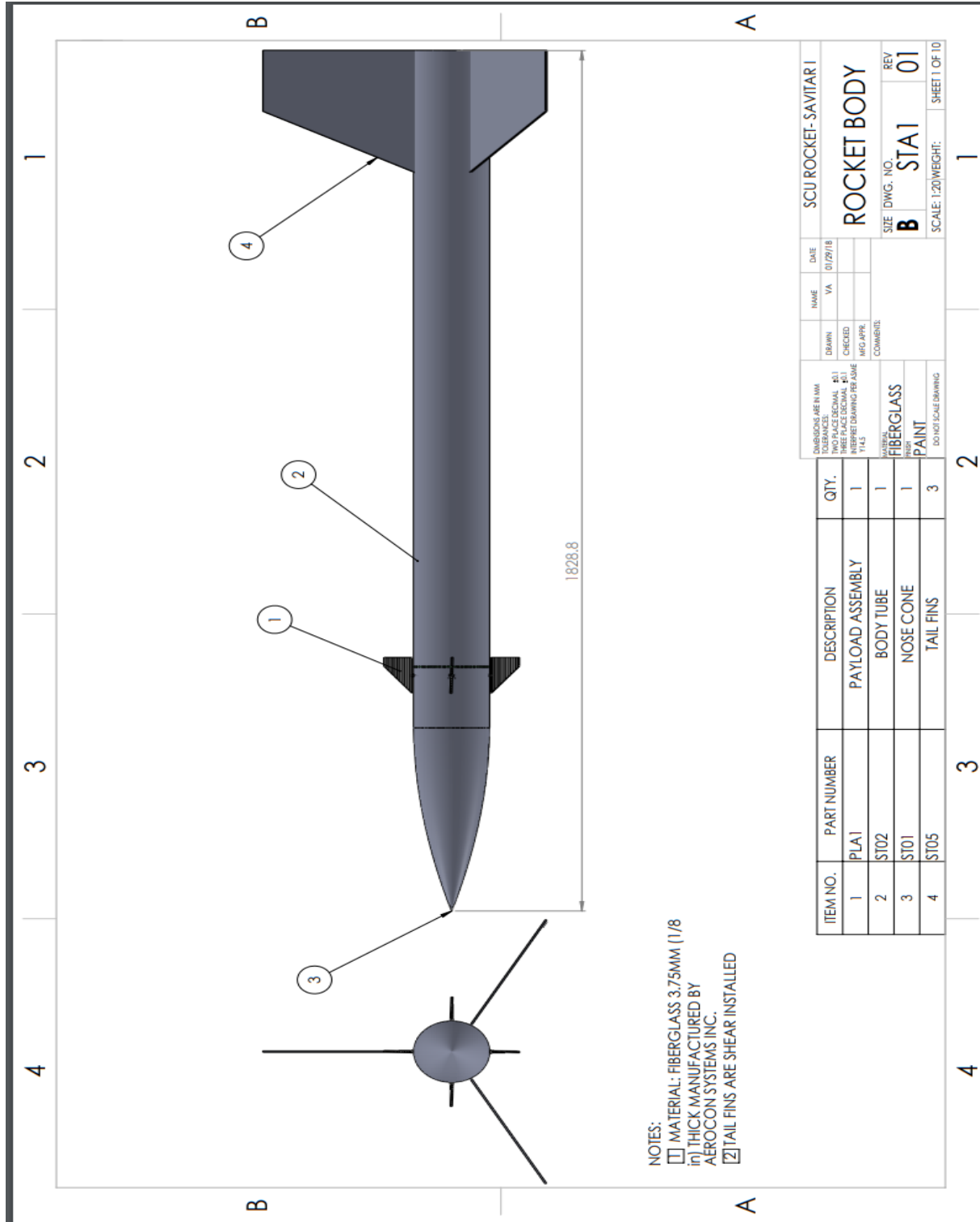
Customer:	Mark Holthaus	Interviewer:	Valeria Avila
Affiliation:	Friends of Amateur Rocketry, Long Beach, CA	Date:	10/22/17
Contact Info:	714-317-4478	Type of User:	Hobbyist, Educator
Question/Prompt	Customer Statement		Interpreted Need
Applications of an active stabilization system?	Rockets are slow when they come off from the launch rail, they fly off with the wind and do not fly straight up; unless the rocket starts at a high velocity.	Rocket to be stabilized once it leaves launch rail, even at slow speeds.	
	It happens every time with slow rockets, defined to have a thrust to weight ratio greater than 1 and less than 3 or under 2 g	Rocket stabilization must work with low thrust to weight ratio rockets. (Thrust to weight ratio: 1-3)	
	The applications could be photographic for those hobbyists that desire to take videos	Rocket must provide stable platform to take pictures or video	
Minimum altitude	It depends on the rocket; if the rocket is heavy, then a good altitude will be required.	Rocket's stabilization must achieve maximum altitude possible with respect to its weight	
Type of stabilization (roll, yaw, pitch)	Roll: this happens very often when launching off the rail, and ruins the rest of the trajectory.	Rocket must not roll	

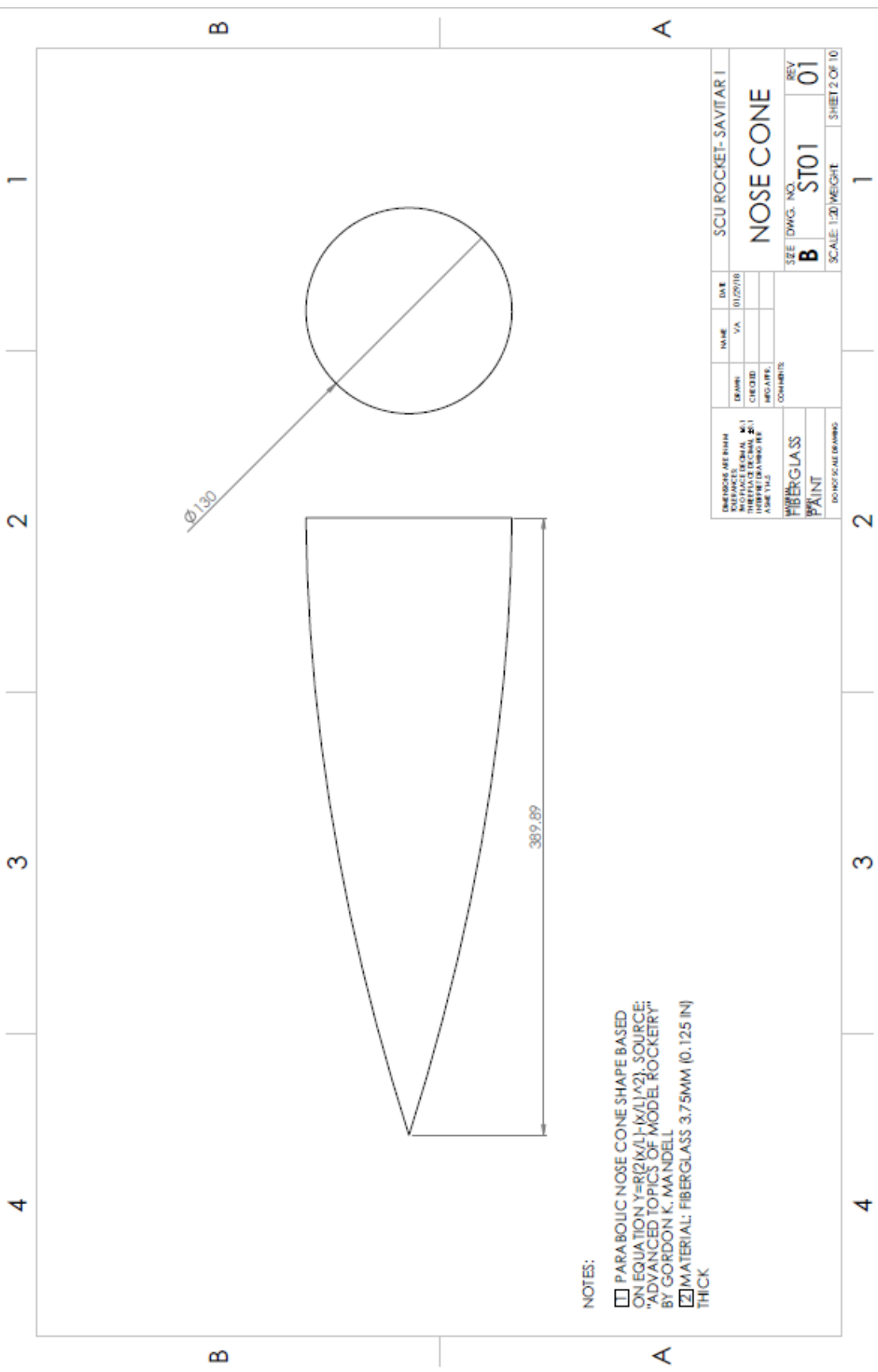
Customer:	Bob Fortune	Interviewer:	Valeria Avila
Affiliation:	Aerocon Systems, San Jose, CA	Date:	10/22/17
Contact Info:	408 272 7001	Type of User:	Hobbyist
Question/Prompt	Customer Statement	Interpreted Need	
Applications of an active stabilization system?	Depends on the cost, complexity and efficacy of the design. Most sounding rockets for the past 60 years have worked fine with fin stabilization.	Rocket can be stabilized no less than previous designs with fin stabilization	
Type of stabilization (roll, yaw, pitch)	Really depends on the payload.	Stabilization agrees with payload's purpose	
Cost	Depends on the efficacy and cost and complexity again. The stabilized military stuff is supremely complex and expensive, but effective.	System's cost agrees with the efficacy and cost.	
	There is a limited amount of space available in a rocket.	Control System fits within the body of the rocket	

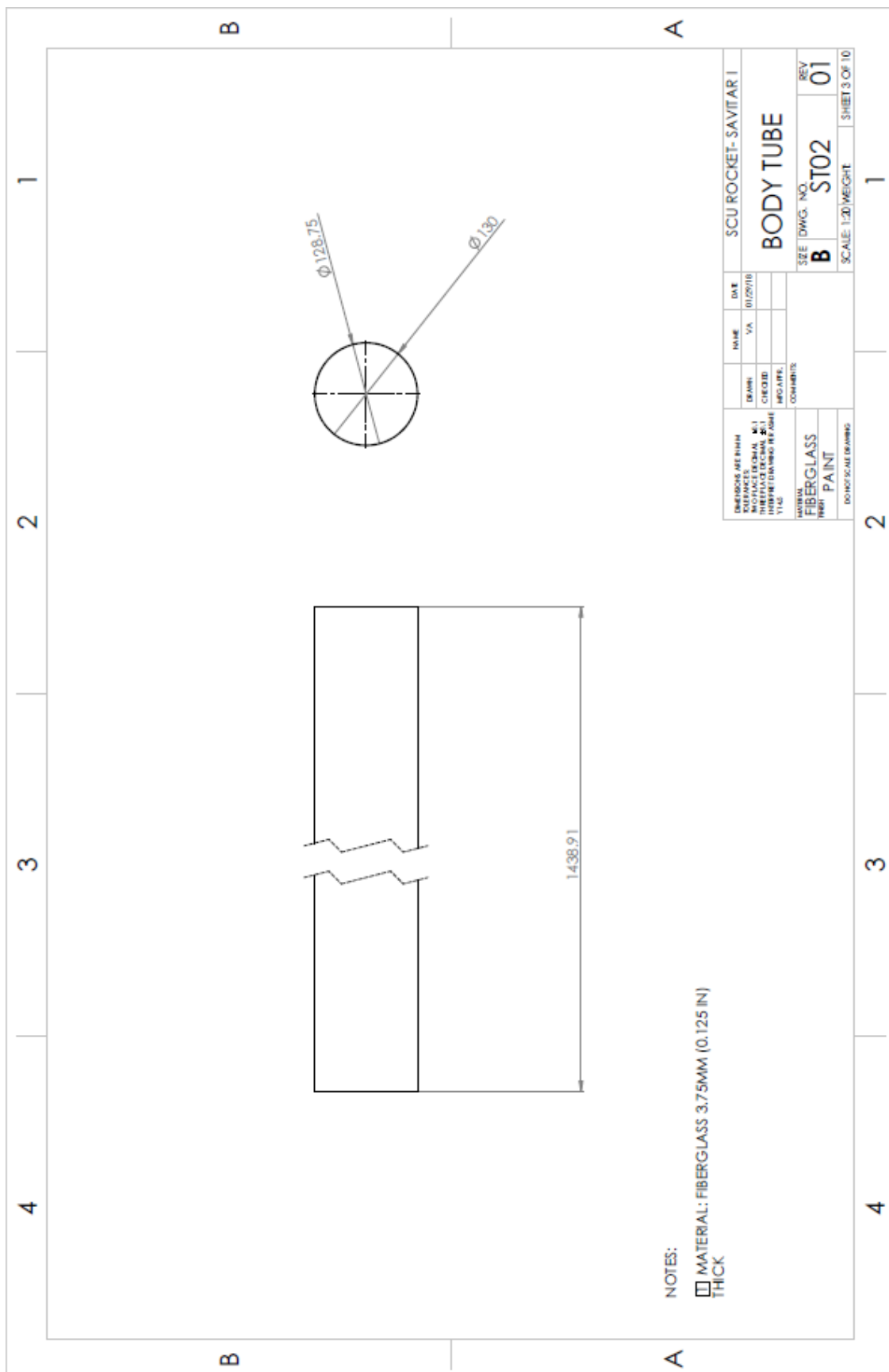
11.2 Appendix B: Project Design Requirements PDS

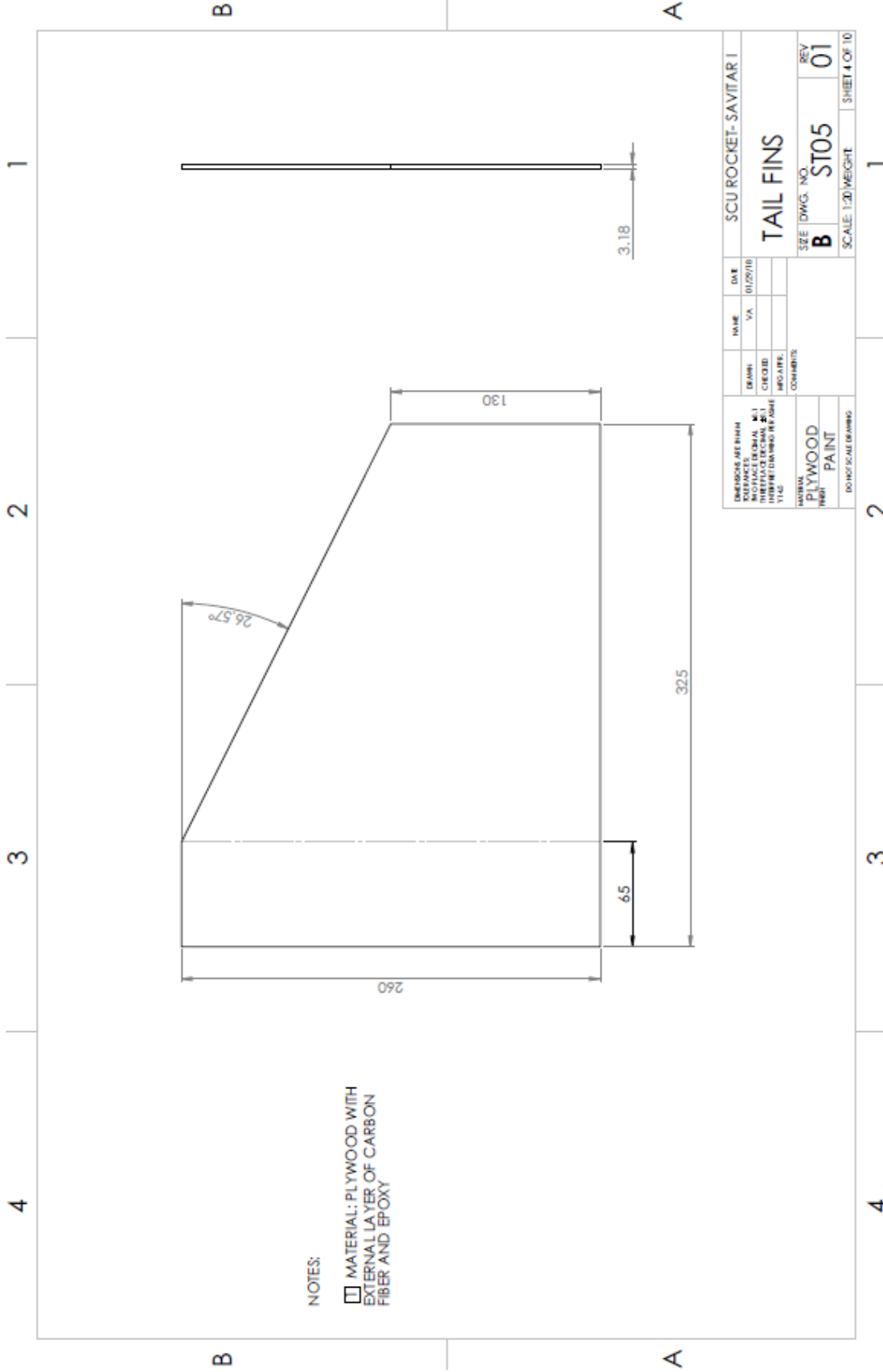
Design Project: Active Control System for Flight Stabilization of High Power Rocket					
Team: Savitar I	Date: April 15th, 2018	Revision: 2			
<u>Datum: Intercollegiate Rocketry Engineering Competition Requirements for 10,000 ft AGL</u>					
<u>and National Fire Protection Association Code for High Power Rocketry 2008</u>					
<u>and 2018 6DOF Simulink Mathematical Model</u>					
ELEMENTS / REQUIREMENTS	Parameters				
	Units	Datum	Target-Range		
System Setup					
Launch Rail PROVIDED BY IREC	[m]	5.5	5.5		
COTS L-N Solid Fuel Motor Total Impulse	[N*s]	<40,960	2,560-20,560		
Motor Diameter	[mm]	54/75	54		
Launch elevation angle	[°]	84 ±1	84 ±1		
System Performance					
Altitude	[m]	3,000	1500-3000+		
Stabilized Roll Rate	[rads/s]	0	±0.12		
Stabilized Pitch Rate	[rads/s]	0	±0.12		
Stabilized Yaw Rate	[rads/s]	0	±0.12		
Vertical Angle	[°]	90	90 ± 5		
Rail departure velocity	[m/s]	>30.5	>30.5		
Stability-Static Margin	[Body Caliber]	1-2	1-2		
Payload-Electronics Bay					
Weight	[kg]	4 ± 5%	4		
Dimension Geometry	[U]	1-3+	1-3+		
Servos Speed	[60 °/s]	0.07	0.06-0.10		
Recovery System					
Deployment	[N/A]	Dual	Single-Dual		
Ejection System	[N/A]	Motor Ejection	Motor Ejection		
Chute Diameter	[m]	2.1	2.1		
Tensile Strength	[N]	98	98		
Descent speed	[m/s]	6	4.5-8.5		
Carrying Capacity at 6mps	[kg]	10	10		
Rocket Structure					
Body Weight	[Kg]	3.4	3.4		
Body Height	[m]	1.83	1.83		
Body Diameter	[cm]	10.18	10 - 15		
Wall Thickness	[mm]	3	3		
Venting Hole	[mm]	3.18-4.76	3.18-4.76		

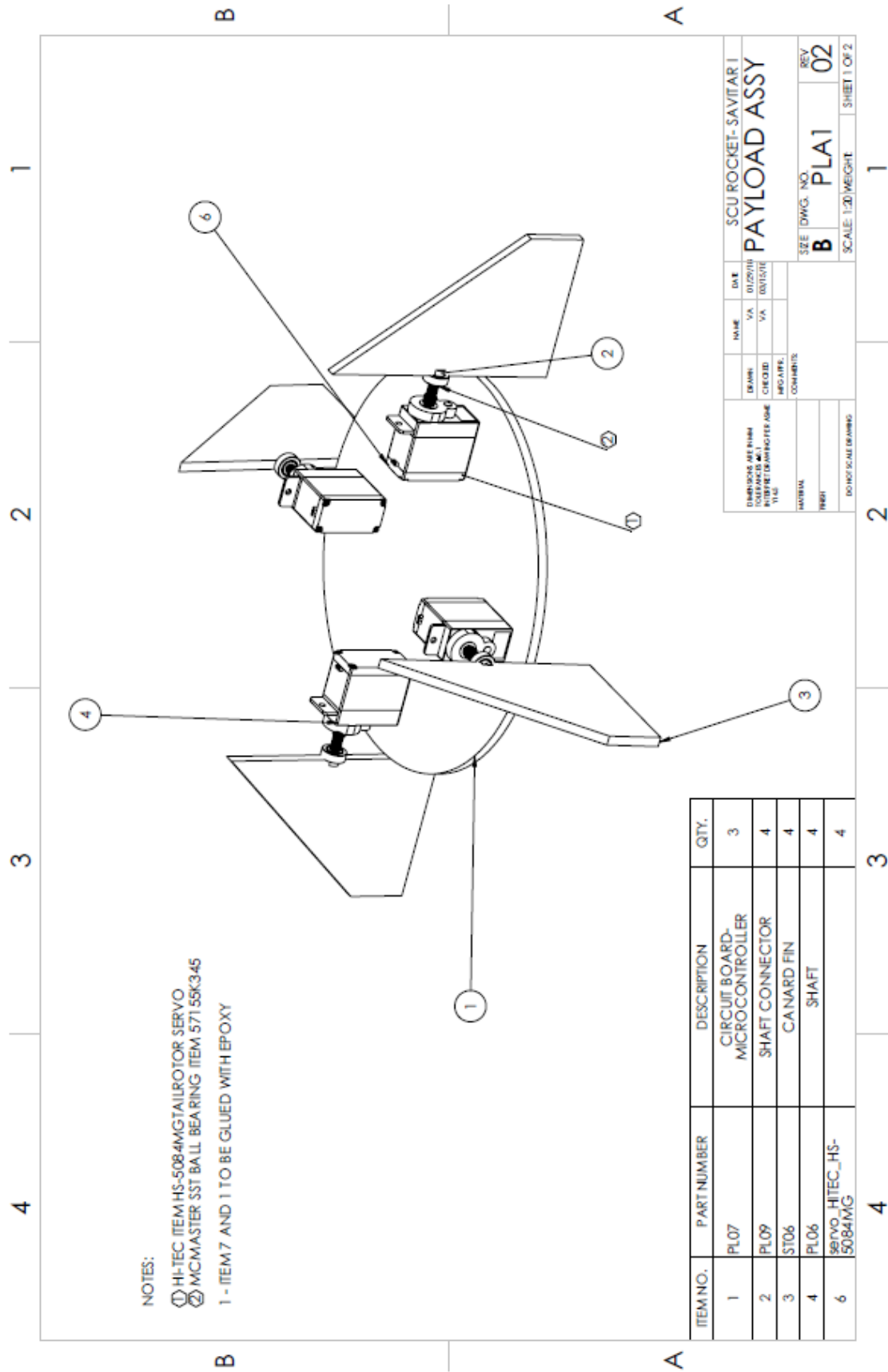
11.3 Appendix C: Assembly Drawings











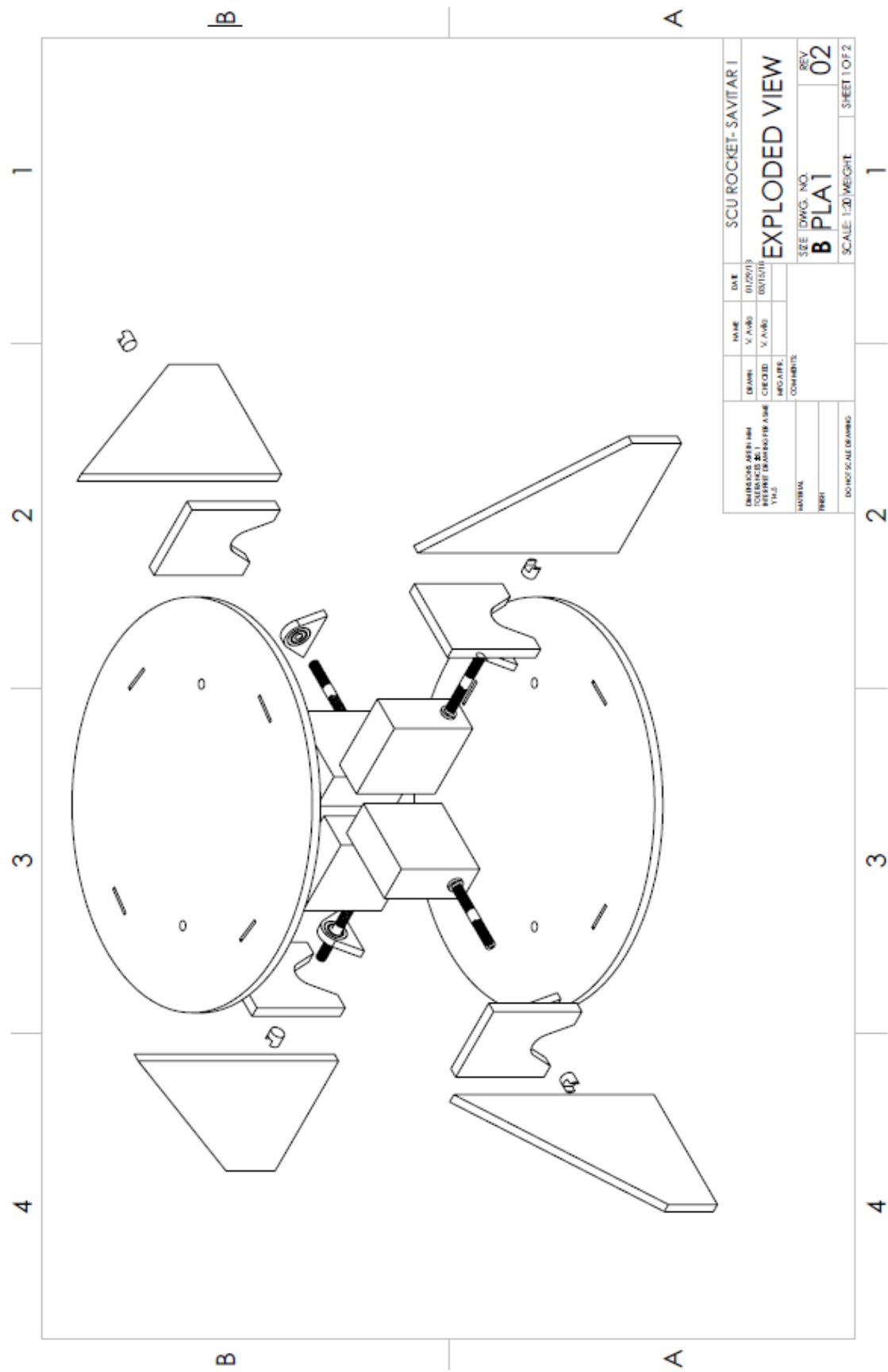
DRAWING MADE BY		NAME		DATE	
DRAFTER: V. A/60		V. A/60		01/29/13	
CHECKED:		V. A/60		01/15/13	
REVIEWED:		V. A/60		01/15/13	
APPROVED:		V. A/60		01/15/13	

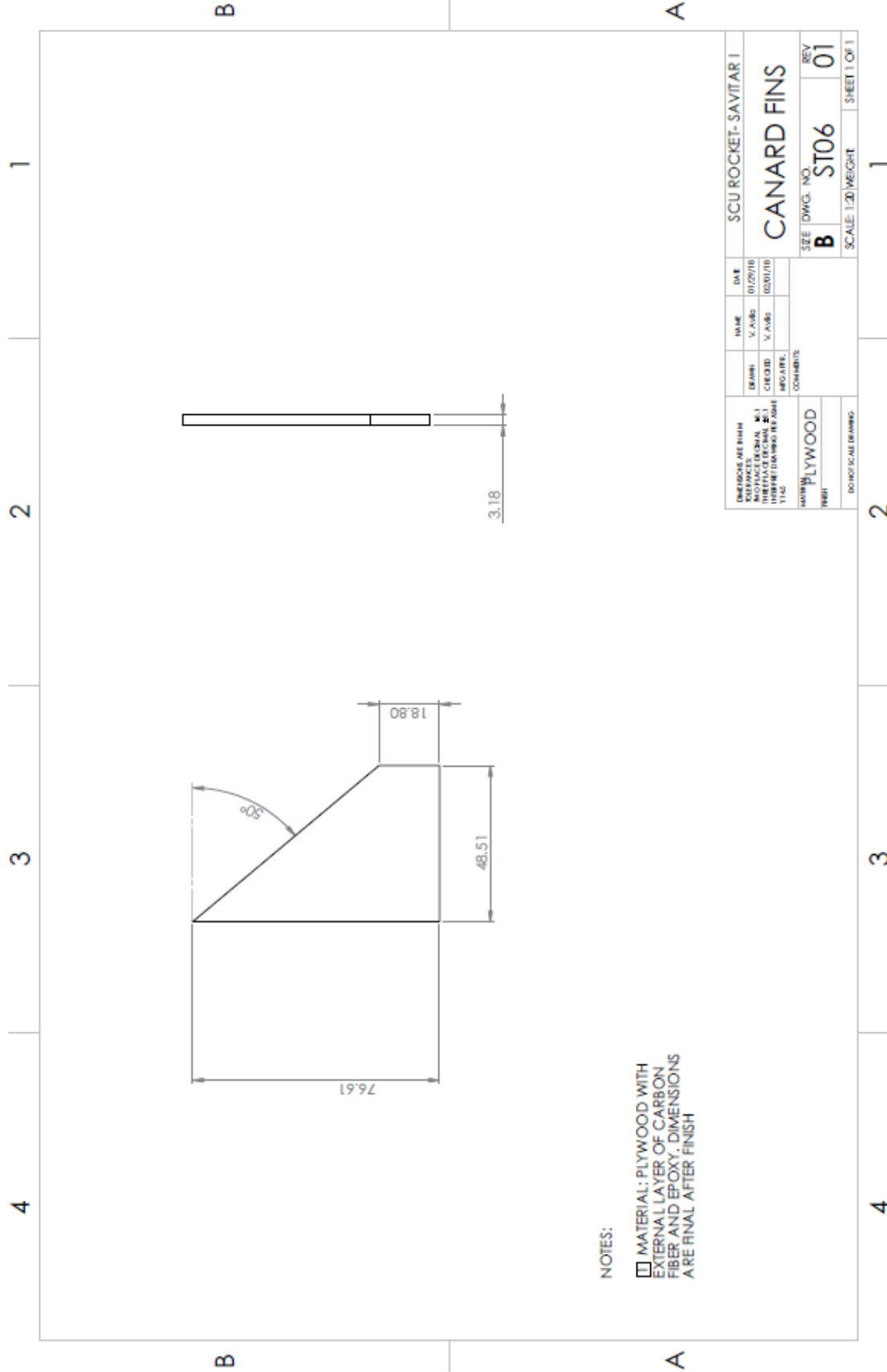
EXPLoded VIEW

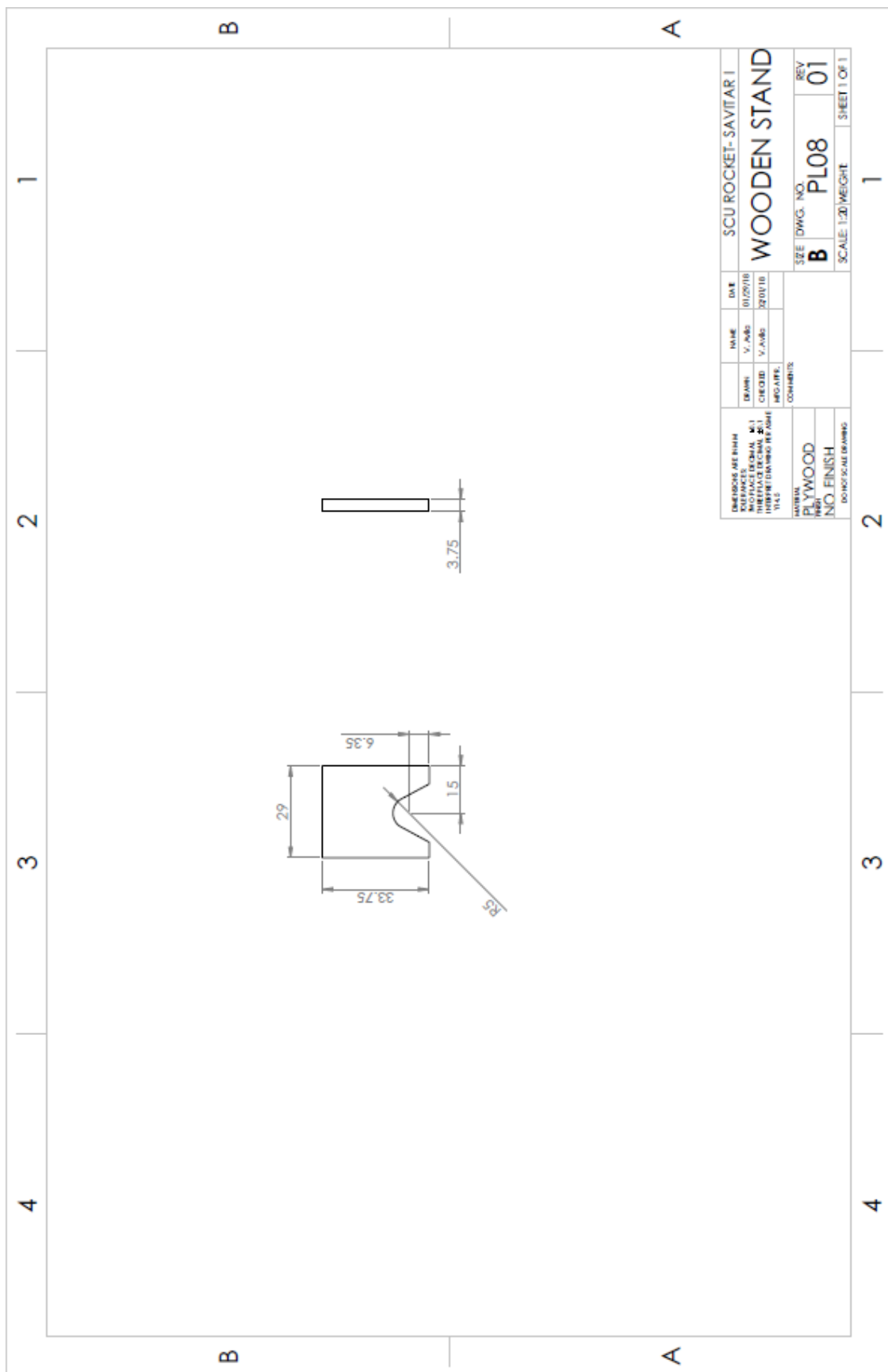
SHEET NO.	REV.
B PLA1	02

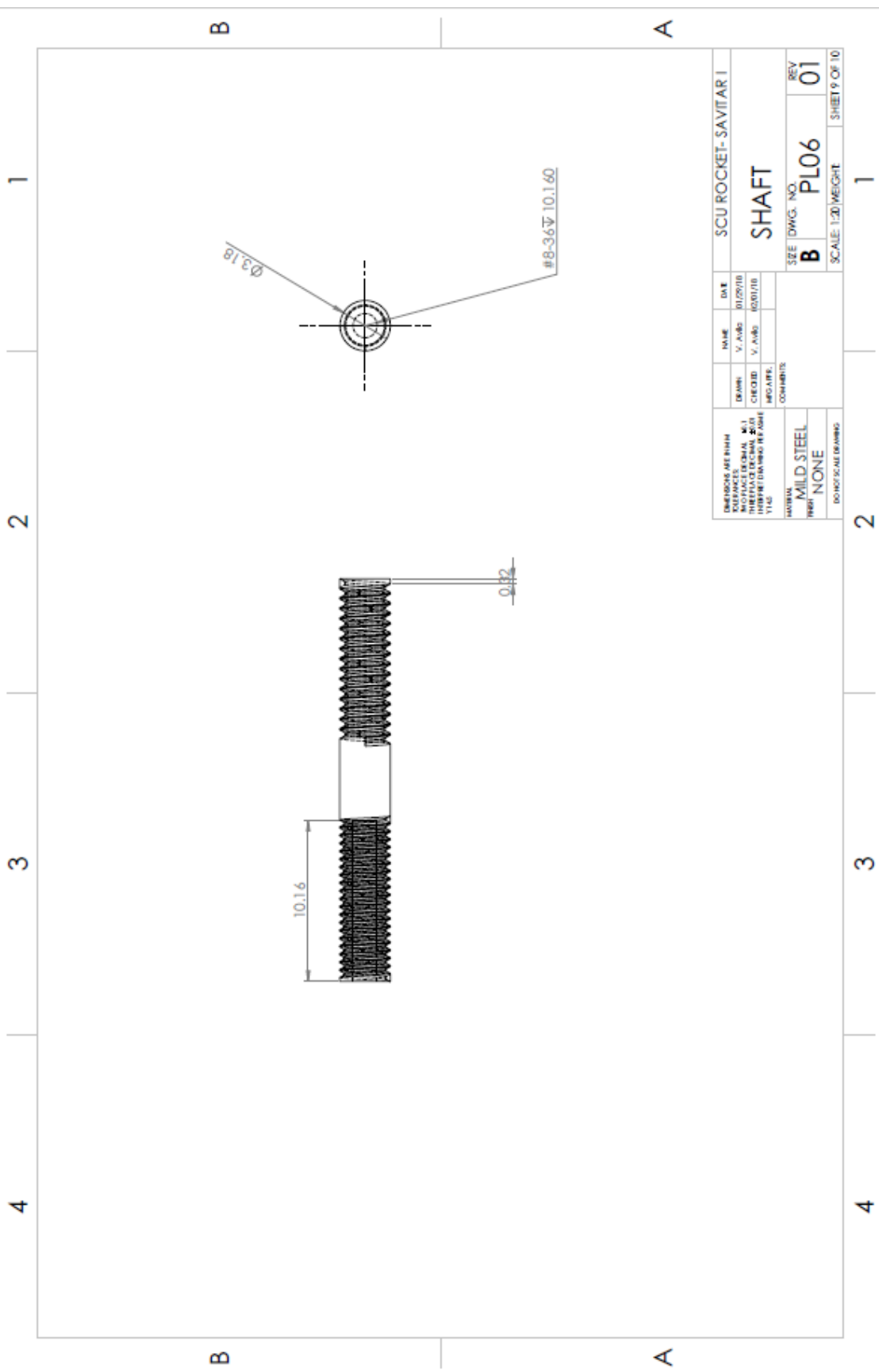
SCALE: 1:20 WEIGHT: 1

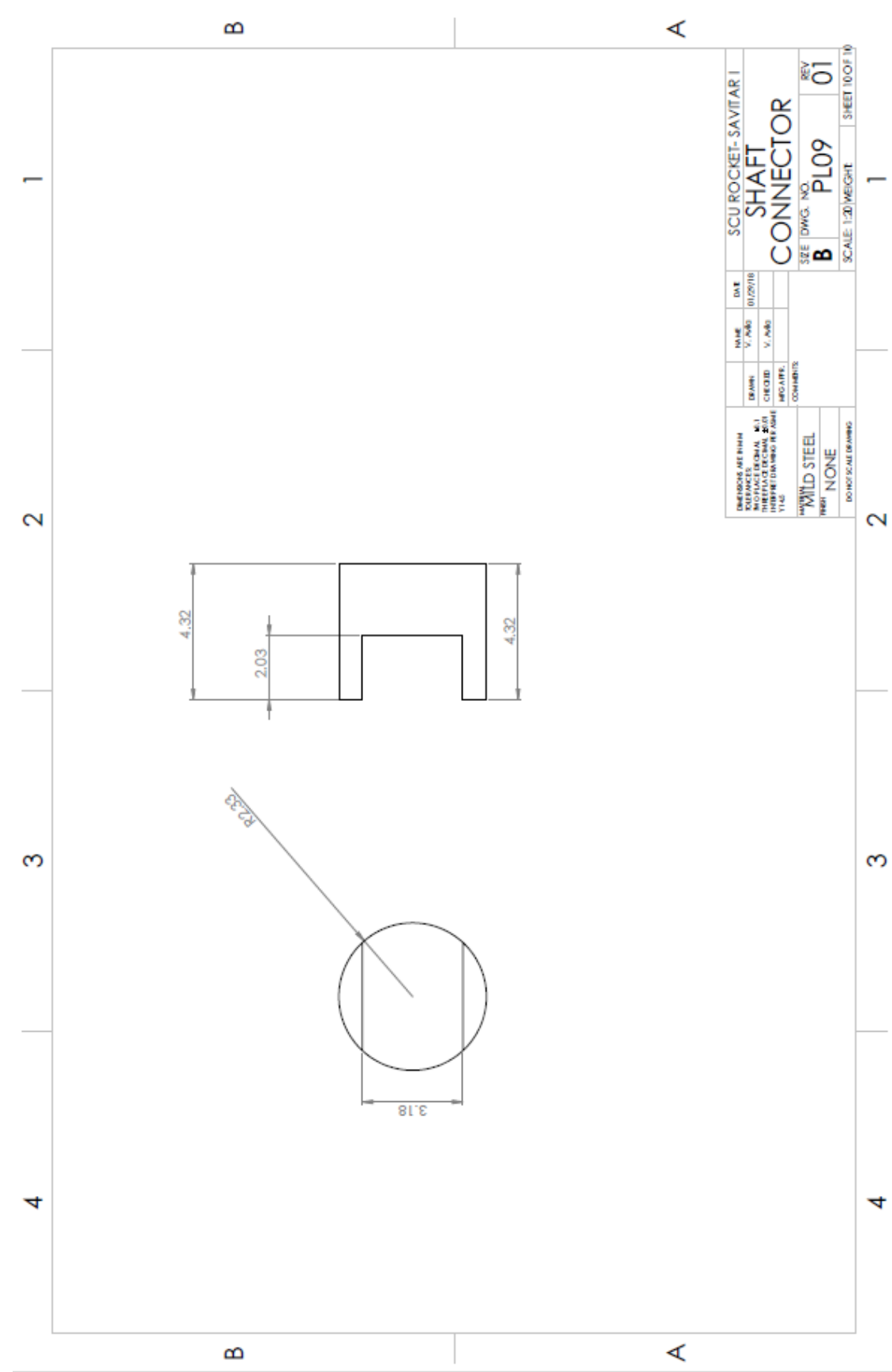
DO NOT SCALE DRAWING











11.4 Appendix D: Senior Design Conference Presentation Slides

SANTA CLARA UNIVERSITY

Active Control System for Flight Stabilization of High-Powered Rocket

Angel Barranco, Daniel Conde, Valeria Avila

Advisor: Dr. Mohammad Ayoubi
Department of Mechanical Engineering

www.scu.edu

ACTIVE CONTROL SYSTEM FOR FLIGHT STABILIZATION

Scu Engineering

SANTA CLARA UNIVERSITY

Outline

- = Motivation and Background
- = Problem Definition
- = Design Process
- = Analysis and Modeling
- = Hardware Implementation and Assembly
- = Next Steps

www.scu.edu

ACTIVE CONTROL SYSTEM FOR FLIGHT STABILIZATION

Scu Engineering

SANTA CLARA UNIVERSITY

Motivation and Background

www.scu.edu

Scu Engineering

SANTA CLARA UNIVERSITY

High Power Rocketry

- = Intercollegiate Rocketry and Engineering Competition
- = Classification
 - Weight greater than 1500 grams
 - Motor weighs more than 125 grams
 - Total Impulse greater than 160 Ns

National Fire Protection Agency High Power Rocket Code 102

Figure 1: Size comparison between sounding rockets.

Scu Engineering

SANTA CLARA UNIVERSITY

Design Requirements

Table 2: Design Requirements based on high power rocketry standards

Requirements	Units	Datum	Target Range
COTS L-M Motor Total Impulse	[N*s]	<50,000	640-5,120
Altitude	[m]	>3,000	3,000-3,500
Stability- Static Margin	(Body Caliber)	>1	1-2
Payload Weight	[kg]	>=4	4
Payload Geometry	[U]	1-3+	1-3+

Datum: Intercollegiate Rocketry Engineering Competition Guidelines

Design Requirements

ACTIVE CONTROL SYSTEM FOR FLIGHT STABILIZATION

Scu Engineering

SANTA CLARA UNIVERSITY

Problem Definition

Scu Engineering

Problem Definition

High power rockets could become dynamically unstable due to outside disturbances such as wind.

GOAL: Active stabilization to eliminate pitch, yaw and roll throughout ascent to maintain a vertical flight path towards apogee.

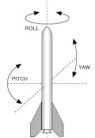


Figure 2: Pitch Yaw and Rolling motion.

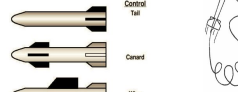
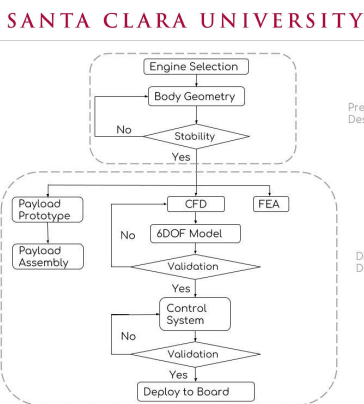


Figure 3: Different methods of controlling a rocket.

Design Process



Engine Selection

Engine Selection

Rocket equation of particle model without drag

$$h_{max} = \frac{1}{2} g_0 I_{sp}^2 \ln^2 \left(\frac{m_0}{m_f} \right) - \frac{g_0 I_{sp}}{m_e} \ln \left(\frac{m_0}{m_f} \right) + \frac{I_{sp} g_0}{m_e} (m_0 - m_f) \quad (1)$$

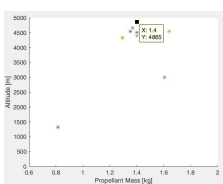


Figure 4: Left: plot showing the relationship between altitude and propellant mass for different motors. Right: plot showing the relationship between altitude and mass flow rate for different motors



Rocket Equation w/ Drag

Rocket equation with drag during burnout

$$\begin{cases} \dot{V} = I_{sp} g_0 \frac{m_0}{m_0 - m_f} - \frac{1}{2} \rho C_D A \frac{V^2}{m_0 - m_f} - g_0 \sin(\gamma) & 0 \leq t \leq t_{burn} \\ h = V \sin(\gamma) & 0 \leq t \leq t_{burn} \end{cases} \quad (2)$$

Rocket equation with drag during coasting

$$\begin{cases} \dot{V} = -\frac{1}{2} \rho C_D A \frac{V^2}{m_0 - m_f} - g_0 \sin(\gamma) & t_{burn} \leq t \leq t_{apogee} \\ h = V \sin(\gamma) & 0 \leq t \leq t_{apogee} \end{cases} \quad (3)$$

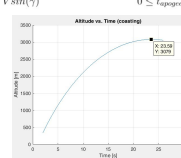


Figure 5: Ascent flight trajectory during coasting phase.

Chosen motor:

L1440 with 2850 Ns total impulse

Initial Sizing: CAD**Dimensions**

- Body
 - = Height: 1.83 m
 - = Diameter: 10.18 cm

Material

- = Skeleton: fiberglass
- = Canard fins: 3D printed with a layer of carbon fiber .

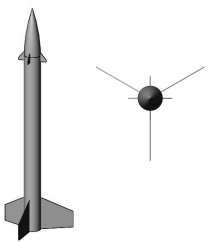
Check stability

Figure 6: CAD model created with geometric dimensions obtained from sizing of motor

Initial Sizing: CAD

ACTIVE CONTROL SYSTEM FOR FLIGHT STABILIZATION

Santa Clara University

7

Analysis and Modeling:**Static and Dynamic Stability**

www.scu.edu

8

Static Stability

- = Determined by center of gravity and center of pressure
 - Wind — Force
 - CG and CP — Moment Arm
 - = w/ rotation around CG
- = Stable Margin: 1-2 Body Calibers

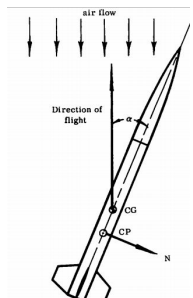


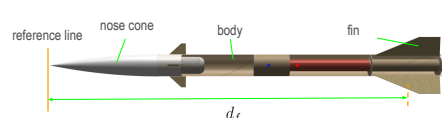
Figure 7: Static Stability Free Body Diagram of Rocket

Analysis and Modeling

ACTIVE CONTROL SYSTEM FOR FLIGHT STABILIZATION

Santa Clara University

9

Center of Gravity - Simplified

$$CG = \frac{d_n W_n + d_b W_b + d_f W_f}{W_R} \quad (4)$$

$d_i \equiv$ distance of component from reference line

$W_i \equiv$ weight of component

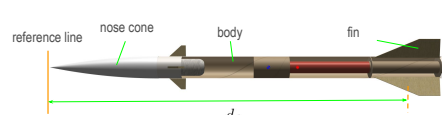
www.scu.edu

10



Center of Gravity: 102 cm

Center of Pressure: 116 cm

Center of Pressure - Simplified

$$CP = \frac{d_n A_n + d_b A_b + d_f A_f}{A_R} \quad (5)$$

$d_i \equiv$ distance of component from reference line

$A_i \equiv$ reference area of rocket

www.scu.edu

11

SANTA CLARA UNIVERSITY

Static Stability - Results

Stability: 1.34 cal

- Center of Gravity: 102 cm
- Center of Pressure: 116 cm

Figure 8: Illustration of 3D rocket model created using OpenRocket

Engine Selection
Initial Sizing: CAD
Analysis and Modeling:

- Stability: Static and Dynamic
- FEA
- CFD

Flight Dynamics:

- 4DOF Model
- Control System

Prototype
Assembly
Testing

www.scu.edu Analysis and Modeling | ACTIVE CONTROL SYSTEM FOR FLIGHT STABILIZATION | Santa Clara University | 13

SANTA CLARA UNIVERSITY

Analysis and Modeling:

Dynamic Stability

www.scu.edu ACTIVE CONTROL SYSTEM FOR FLIGHT STABILIZATION | Santa Clara University | 14

SANTA CLARA UNIVERSITY

Ideal Damping

Engine Selection
Initial Sizing: CAD
Analysis and Modeling:

- Stability: Static and Dynamic
- FEA
- CFD

Flight Dynamics:

- 4DOF Model
- Control System

Prototype
Assembly
Testing

www.scu.edu Analysis and Modeling | ACTIVE CONTROL SYSTEM FOR FLIGHT STABILIZATION | Santa Clara University | 15

SANTA CLARA UNIVERSITY

Cases Analyzed

Engine Selection
Initial Sizing: CAD
Analysis and Modeling:

- Stability: Static and Dynamic
- FEA
- CFD

Flight Dynamics:

- 4DOF Model
- Control System

Prototype
Assembly
Testing

= Homogeneous

- No disturbances

= Step

- Inputs a disturbance
 - Discontinuous wind shear
 - Accidental Angled Takeoff
 - Deflection on Opposing Tail Fins

www.scu.edu Analysis and Modeling | ACTIVE CONTROL SYSTEM FOR FLIGHT STABILIZATION | Santa Clara University | 16

SANTA CLARA UNIVERSITY

Solutions

Homogeneous Response

Step Response

$\alpha_x = Ae^{-Dt} \sin(\omega t + \phi)$

Figure 9: Underdamped homogeneous response.

Damping Ratio: $0.82 \leq \zeta \leq 0.89$

Figure 10: Underdamped step response.

Step Input: 0.222

Engine Selection
Initial Sizing: CAD
Analysis and Modeling:

- Stability: Static and Dynamic
- FEA
- CFD

Flight Dynamics:

- 4DOF Model
- Control System

Prototype
Assembly
Testing

www.scu.edu Analysis and Modeling | ACTIVE CONTROL SYSTEM FOR FLIGHT STABILIZATION | Santa Clara University | 17

SANTA CLARA UNIVERSITY

Ways to Reduce Damping Ratio

Engine Selection
Initial Sizing: CAD
Analysis and Modeling:

- Stability: Static and Dynamic
- FEA
- CFD

Flight Dynamics:

- 4DOF Model
- Control System

Prototype
Assembly
Testing

= Reduce fin planform area

= Increase rocket's weight and/or length

= Moving fins closer to CG

www.scu.edu Analysis and Modeling | ACTIVE CONTROL SYSTEM FOR FLIGHT STABILIZATION | Santa Clara University | 18



Analysis and Modeling:

Finite Element Analysis



Mode Number and Natural Frequency

Table 3: Natural frequencies at each mode number for the rocket.

Mode	Frequency (Hz)
1	0
2	7.05E-4
3	1.36E-3
4	2.78E-2
5	0.21
6	1.37

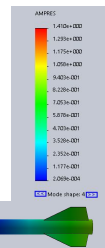


Figure 11: Resulting Amplitude of Mode 6



Analysis and Modeling:

Computational Fluid Dynamics



Purpose

- = Yield Better Understanding of the Flow Around the Body
 - Verification of Assuming Subsonic Speed
- = Design Canard Fins
 - Study drag effects on body
- = Aerodynamic Coefficients
 - Static, dynamic and control derivatives

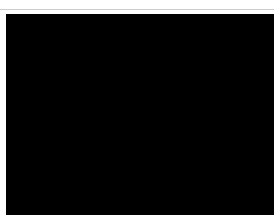
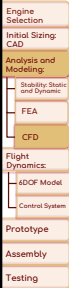


Figure 12: CFD Mach Number Analysis



Profile Comparison

- = Clipped Delta Shape
 - Lowest drag at zero angle of attack
- = Differences
 - More rounded leading edge
 - Majority of mass is at the beginning of chord line than middle
 - Trailing edge unsharpened
- = Reasoning
 - Difficulty in manufacturing
 - Defects in 3D printing at the leading and trailing edge

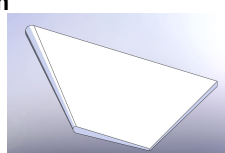


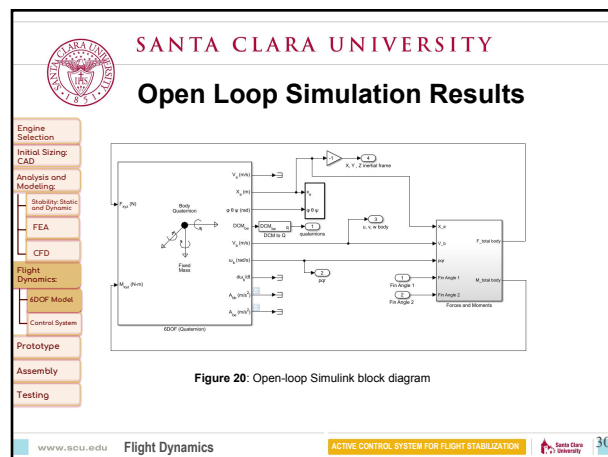
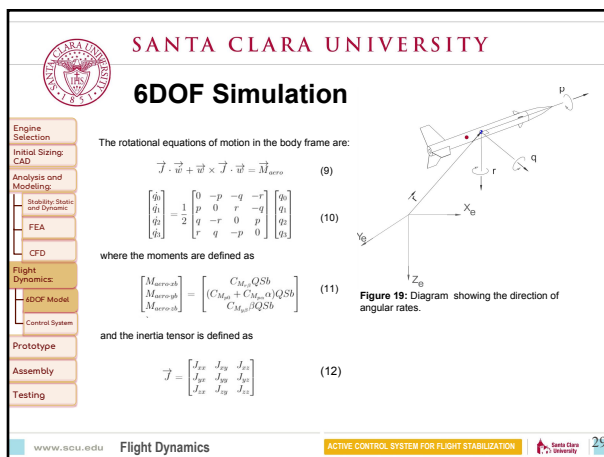
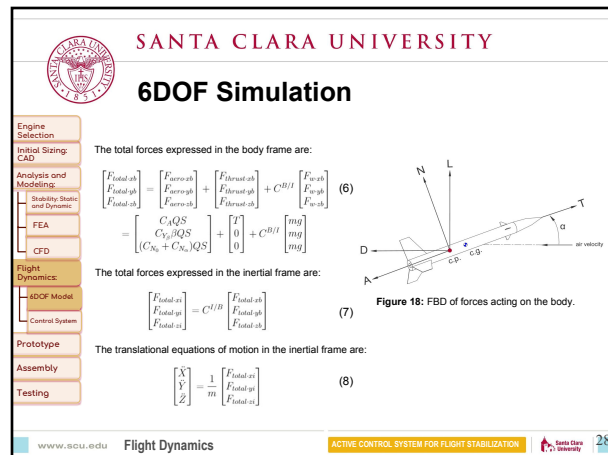
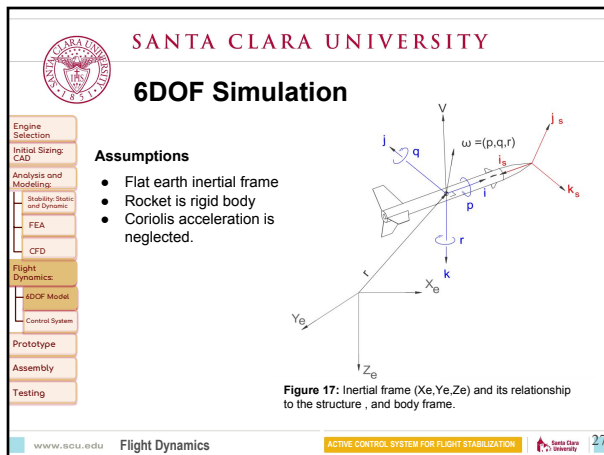
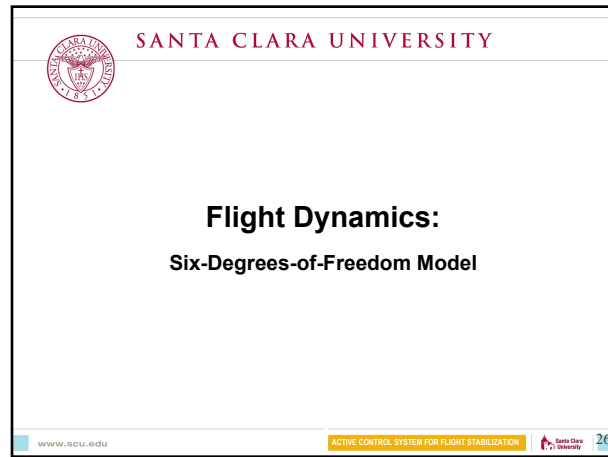
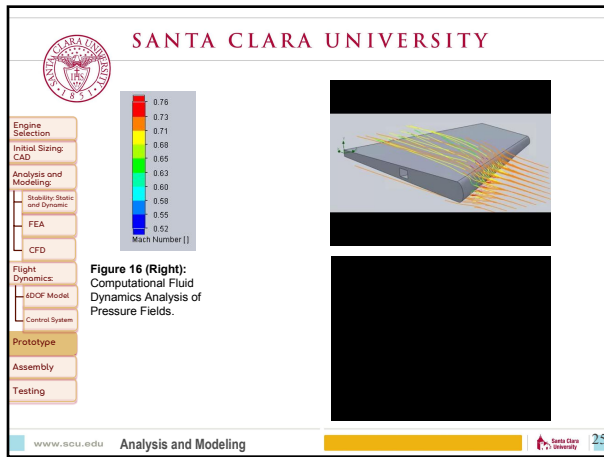
Figure 13: Isometric profile view of canard fin.

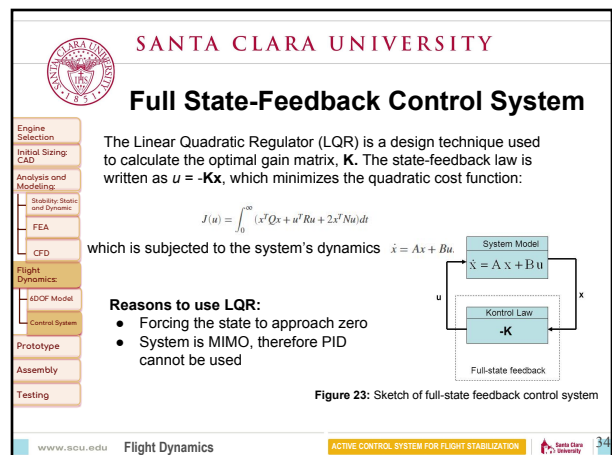
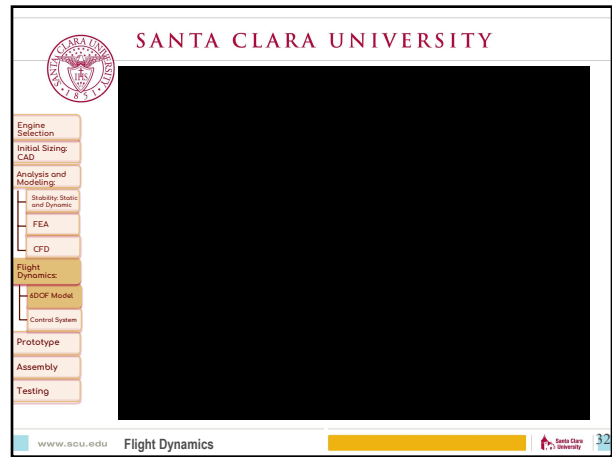
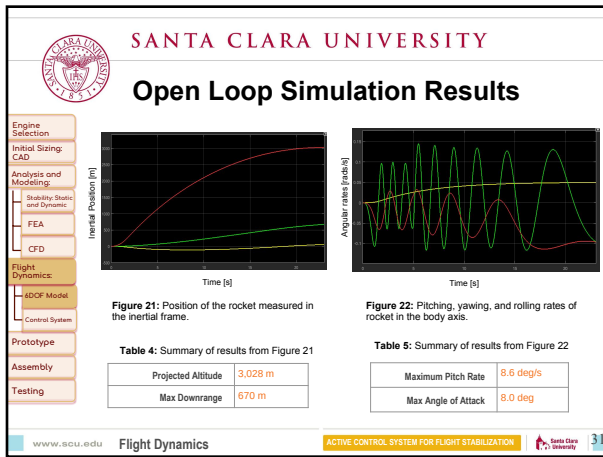
Symmetrical airfoil

Figure 14: Side profile view of generic airfoil.



Figure 15: Side profile view of canard fin.





SANTA CLARA UNIVERSITY

Hardware Conceptual Design

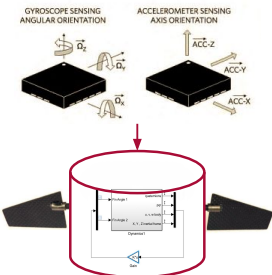


Figure 26: Conceptual Design

- Engine Selection
- Initial Sizing: CAD
- Analysis and Modeling:
 - Stability, Static and Dynamic
 - FEA
 - CFD
- Flight Dynamics:
 - 4DOF Model
 - Control System
- Prototype
- Assembly
- Testing

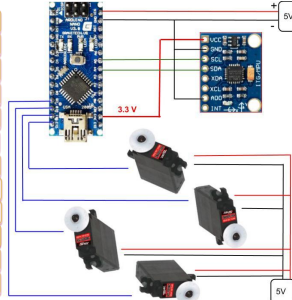
www.scu.edu Hardware Implementation

ACTIVE CONTROL SYSTEM FOR FLIGHT STABILIZATION

37

SANTA CLARA UNIVERSITY

Construction of Control Hardware



- = 1x IMU 6DOF MPU6050
 - Gyroscope
 - Accelerometer
- = 1x Arduino Nano Board
 - Up to 16 MHz Clockspeed
- = 4x Hitec HS5084MG
 - Digital Servos, Metal Gears
 - 3-pole Bearing Type
 - (4.8V/6.0V) 21/26 Torque kg/cm

www.scu.edu Hardware Implementation

ACTIVE CONTROL SYSTEM FOR FLIGHT STABILIZATION

38

SANTA CLARA UNIVERSITY

Payload Design

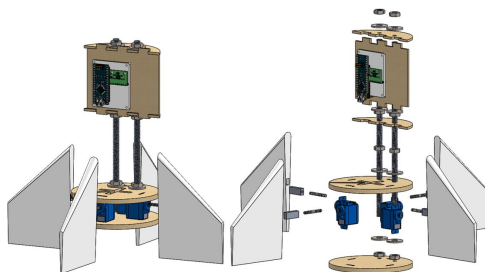


Figure 27: CAD Rendering and exploded view of payload detail design

- Engine Selection
- Initial Sizing: CAD
- Analysis and Modeling:
 - Stability, Static and Dynamic
 - FEA
 - CFD
- Flight Dynamics:
 - 4DOF Model
 - Control System
- Prototype
- Assembly
- Testing

www.scu.edu Hardware Implementation

ACTIVE CONTROL SYSTEM FOR FLIGHT STABILIZATION

39

SANTA CLARA UNIVERSITY

Control Hardware Prototype

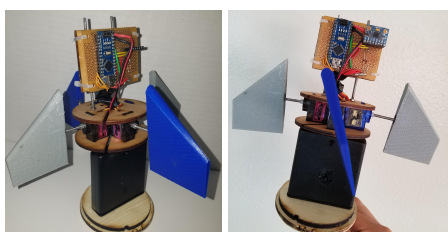


Figure 28 (left and right): Hardware Prototype

www.scu.edu Hardware Implementation

ACTIVE CONTROL SYSTEM FOR FLIGHT STABILIZATION

40

SANTA CLARA UNIVERSITY

Control Hardware Prototype



Figure 32: Test of the Hardware Prototype Electronics

- Engine Selection
- Initial Sizing: CAD
- Analysis and Modeling:
 - Stability, Static and Dynamic
 - FEA
 - CFD
- Flight Dynamics:
 - 4DOF Model
 - Control System
- Prototype
- Assembly
- Testing

www.scu.edu Hardware Implementation

ACTIVE CONTROL SYSTEM FOR FLIGHT STABILIZATION

41

SANTA CLARA UNIVERSITY

Hardware Testing

- = Deploy finalized controller to hardware
 - Compile Simulink Controller into C code using Embedded Coder
 - Deploy verified code into Arduino platform
- = Calibration of sensors
- = Test response of the controller

www.scu.edu Hardware Implementation

ACTIVE CONTROL SYSTEM FOR FLIGHT STABILIZATION

42



Verification and Validation



Assembly



Building the Rocket



Figure 31: Final Payload with Teensy microcontroller and final rocket



Meeting Specifications

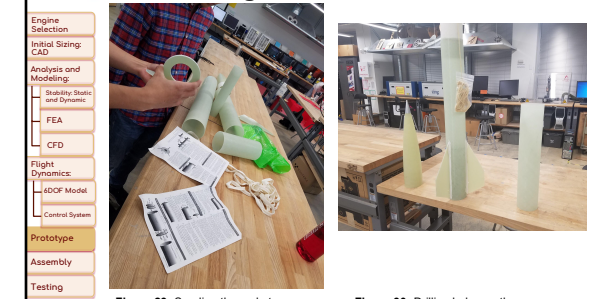
Table 6: Design specifications for the project with current values.

Requirements	Units	Datum	Target Range	Current Values
COTS L-M Motor Total Impulse	[N*s]	<50,000	640-5,129	2,850 ✓
Altitude	[m]	>3,000	3,000-3,500	3,079 ✓
Stability- Static Margin	[Body Caliber]	>1	1-2	1.34 ✓
Payload Weight	[kg]	>=4	4	.750
Payload Geometry	[U]	1-3+	1-3+	1.5 ✓

Datum: Intercollegiate Rocketry Engineering Competition Guidelines



Building the Rocket



Next Steps

- = Deploy finalized controller to hardware
- = Add altimeter data logging to payload
- = Launch test with and without stabilization system
- = Analysis of experimental and modeled data



Thank You



Questions?



Equations

Homogeneous:

$$I_L \left(\frac{d^2 \alpha_x}{dt^2} \right) + C_2 \left(\frac{d \alpha_x}{dt} \right) + C_1 \alpha_x = 0 \quad (6)$$

Step:

$$I_L \left(\frac{d^2 \alpha_x}{dt^2} \right) + C_2 \left(\frac{d \alpha_x}{dt} \right) + C_1 \alpha_x = 0 \quad (t < 0) \quad (7)$$

$$I_L \left(\frac{d^2 \alpha_x}{dt^2} \right) + C_2 \left(\frac{d \alpha_x}{dt} \right) + C_1 \alpha_x = M_s \quad (t \geq 0) \quad (8)$$

Coefficients:

$$C_1 = \frac{1}{2} \rho V(t)^2 A_{r,fm} C_N (X_{CP} - X_{CG}) \quad (9)$$

$$C_2 = \frac{1}{2} \rho V(t)^2 A_{r,fm} [C_{N,fm}(Z_{fm} - X_{CG})^2 + C_{N,cone}(Z_{cone} - X_{CG})^2] + \dot{m}(Z_{cone} - X_{CG})^2 \quad (10)$$



Equations

Coefficients:

$$C_1 = \frac{1}{2} \rho V(t)^2 A_{r,fm} C_N (X_{CP} - X_{CG}) \quad (9)$$

$$C_2 = \frac{1}{2} \rho V(t)^2 A_{r,fm} [C_{N,fm}(Z_{fm} - X_{CG})^2 + C_{N,cone}(Z_{cone} - X_{CG})^2] + \dot{m}(Z_{cone} - X_{CG})^2 \quad (10)$$



Damping Ratio

Equation

$$\zeta = f(V(t)) \quad \zeta = \frac{C_2}{2\sqrt{C_1 I_L}}$$



Calculations of Drag and Axial Force Coefficient of Rocket

Results:

$$C_D = 0.57 \quad C_A = -3.24$$

Method:

$$C_D = \frac{F}{\frac{1}{2} \rho V^2 A_r}$$

$$C_A = \frac{C_D \cos(\alpha) - \frac{1}{2} C_N \sin(2\alpha)}{1 - \sin^2 \alpha}$$

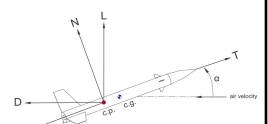


Figure 38: Free-Body Diagram of Forces on a Rocket

$$\vec{F} = \int P(\vec{n}) dA$$

$$C_D = C_{D,cone} + C_{D,body} + C_{D,fins} + C_{D,interference}$$



SANTA CLARA UNIVERSITY

Construction of Control Hardware



Engine Selection
Initial Sizing:
CAD
Analysis and Modeling:
- Statics: Static and Dynamic
- FEA
CFD
Flight Dynamics:
- 4DOF Model
Control System
Prototype
Assembly
Testing

Hardware Implementation

ACTIVE CONTROL SYSTEM FOR FLIGHT STABILIZATION

55



SANTA CLARA UNIVERSITY

Closed-Loop Simulation Results

Engine Selection
Initial Sizing:
CAD
Analysis and Modeling:
- Statics: Static and Dynamic
- FEA
CFD
Flight Dynamics:
- 4DOF Model
Control System
Prototype
Assembly
Testing

poles =

```

0.4050 + 0.0001i -> -22.3777 + 42.2989i
0.4050 - 0.0001i -> -22.3777 - 22.2990i
-0.0071 + 6.7118i -> -22.9980 + 42.3246i
-0.0071 - 6.7118i -> -22.9980 - 42.3246i
-0.4568 + 0.0001i -> -1.9986 + 0.00001i
-0.4568 - 0.0001i -> -1.9986 - 0.00001i
-0.1375 + 0.00001i -> -0.1835 + 0.1575i
-0.1375 - 0.00001i -> -0.1835 - 0.1575i
-0.0215 + 1.4558i -> -0.0907 + 0.0846i
0.0215 - 1.4558i -> 0.0907 - 0.0846i
0.0402 + 0.0001i -> 0.0446 + 0.00001i
0.0402 - 0.0001i -> 0.0446 - 0.00001i
0.0042 + 0.0245i -> 0.0718 - 0.0558i
0.0042 - 0.0245i -> -0.0532 + 0.00001i
-0.0008 + 0.0001i -> -0.0134 + 0.00002i

```

pole_cont =

```

-22.3777 + 42.2989i
-22.3777 - 22.2990i
-22.9980 + 42.3246i
-22.9980 - 42.3246i
-1.9986 + 0.00001i
-1.9986 - 0.00001i
-0.1835 + 0.1575i
-0.1835 - 0.1575i
-0.0907 + 0.0846i
0.0907 - 0.0846i
0.0446 + 0.00001i
0.0446 - 0.00001i
0.0718 - 0.0558i
-0.0532 + 0.00001i
-0.0134 + 0.00002i

```

K =

```

1.0e+05 *

```

```

-0.0947 0.0137 0.1129 -0.1026 0.4619 -0.0001 0.0000 0.0001 -0.0002 -0.0003 -0.0000 -0.0000 0.0000
-0.1236 -0.0611 0.1443 -0.0833 -0.4754 -0.0000 0.0001 0.0003 -0.0002 -0.0004 -0.0000 -0.0000 -0.0002

```

Figure 24: (Right) open-loop poles.
(left) closed-loop poles.

Figure 25: Simulink block diagram of closed-loop system

Figure 26: Gain matrix, K

www.scu.edu Flight Dynamics

ACTIVE CONTROL SYSTEM FOR FLIGHT STABILIZATION

Santa Clara University

56



SANTA CLARA UNIVERSITY

Budget

Components	Budget
Off-the-shelf M-Motor	\$250.00
Off-the-shelf rocket	\$560.00
Manufacturing materials: plywood, carbon fiber,	\$110.00
Electronics	\$100.00
Actuators	\$300.00
TOTAL	\$1,320
LEFT	\$0

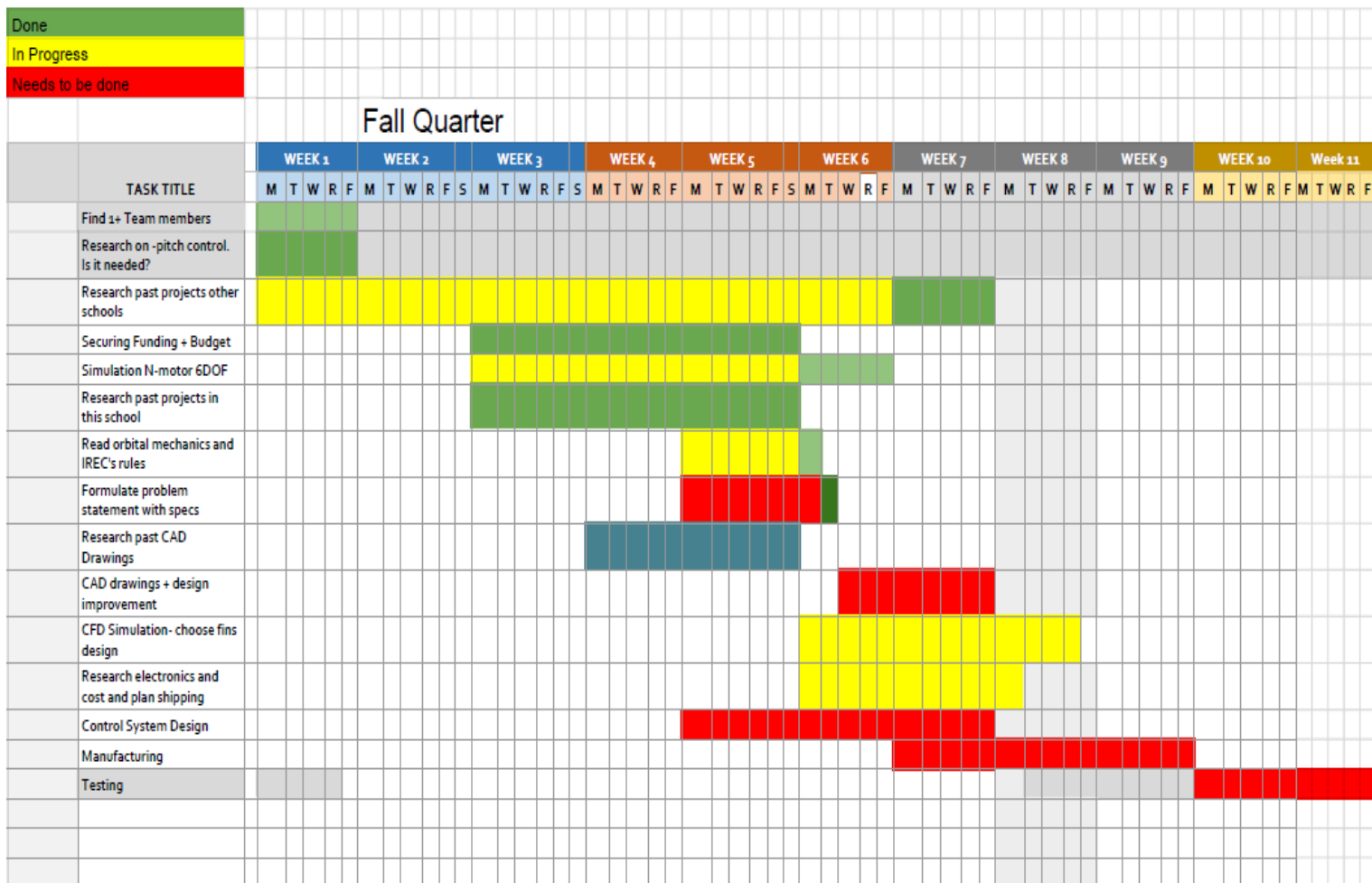
www.scu.edu

Flight Dynamics

ACTIVE CONTROL SYSTEM FOR FLIGHT STABILIZATION

57

11.5 Appendix E: Gantt Chart



Done
In Progress
Needs to be done

Winter Quarter

CODE	TASK TITLE	PHASE ONE			PHASE TWO			PHASE THREE			PHASE FOUR													
		WEEK 1	WEEK 2	WEEK 3	WEEK 4	WEEK 5	WEEK 6	WEEK 7	WEEK 8	WEEK 9	WEEK 10													
M	T	W	R	F	M	T	W	R	F	M	T	W	R	F	M	T	W	R	F	M	T	W	R	F
	Find dimensions and location of canard fins																							
	Body dimensions + order																							
	Order body																							
	CAD																							
	CFD																							
ME195	Revised schedule/Parts List																							
ME195	Budget Update																							
ME195	Detail Drawing																							
	Vibrations																							
	Designing CS and circuit board hardware																							
ME195	Analysis Report/Oral Presentations																							
	Individual testing of control system																							
ME195	Formal written and oral progress report																							
	Testing of full assembly																							
ME195	Assembly drawings																							
	Interpretation of data																							
	Fix anything broken/Make improvements																							

		Spring Quarter																							
CODE	TASK TITLE	WEEK 1		WEEK 2		WEEK 3		WEEK 4		WEEK 5		WEEK 6		WEEK 7		WEEK 8		WEEK 9		WEEK 10		Week 11			
		M	T	W	R	F	M	T	W	R	F	S	M	T	W	R	F	M	T	W	R	F	M	T	W
STR	Build Rocket Prototype																								
STR	Assembly Prototype																								
ME196	Thesis ch 4 and Table of Contents.																								
ME196	Gather receipts for refund																								
PLA	finalize prototype control code																								
PLA	Payload assembly with hardware																								
PLA	Testing of payload																								
PLA	Mode Shapes/ Dynamic Response																								
STR	Manufacturing Fins																								
STR	Test Carbon Fiber																								
STR	Assembly Final Rocket-eyebolt, rail buttons, bulkhead pressure,																								
TEST	First Test Lz Cert																								
TEST	Launch																								
PLA	Test Camera																								
ME196	PDS Update, Experimental Protocol																								
CS	Build controller in simulink and export model to arduino																								
SoE	Poster Board Due SEEDS																								
SoE	SEEDS Showcase																								
CS	Tuning Control System																								
	Add altimeter																								
	Dual deployment prep																								
TEST	Second Test Lz Cert																								
ME196	Senior Design Conference and practice presentations																								
ME196	Draft Thesis																								
ME196	Patent Search/Business Plan																								
ME196	Open house																								
ME196	Thesis Due																								

11.6 Appendix F: Business Plan

Santa Clara University School of Engineering



SAVITAR I: Active Control Stabilizing System for Model Rockets

Business Plan

Valeria Avila

Angel Barranco

Daniel Conde

June 8, 2018

Abstract

The plan is to develop a product for the amateur community. This product will facilitate any research and/or educational practices that come with the use of sounding rockets. This product will be easy to use, and will use minimal assembly steps. In addition, the product will require little to no knowledge about electronics or programming in order to use it properly and effectively. Lastly, but most importantly, the product will follow ITAR regulations in order to make sure that the product does not violate any federal laws.

Table of Contents

Introduction	4
Goals and objectives of the company	4
Product Description	4
Potential markets	5
Service or warranties	5
Financial plan and investor's return on investment (ROI)	Error! Bookmark not defined.

Introduction

The product dimensions will be about 4 inches in diameter, and 8 inches long. This will be the standard size, but modifications to the system could be easily made so that the control system could fit in any high power rocket body structure. The team believes that this is imperative since amateur rocketry is already an expensive hobby, and hobbyists are not going to be willing to buy a control system for every rocket size they have. The market for this product is very narrow since it will target to just amateur rocketry. On top of that, not every amateur rocketry will see the need for this product. As of right now, the team believes that the total personnel needed to create an effective product is 4: Sales representative, test engineer, mechatronics engineer, and manufacturing engineer. The sales representative would be tasked with processing all the invoices and accounting. The test engineer would be mainly responsible for testing the hardware and software to make sure the control system is operating properly without any flaws. The mechatronics engineers would be responsible for research and development to always keep improving the product. Lastly, the manufacturing engineer would be in charge of manufacturing specific components for the control system to make sure they meet the needs of the product.

The competition for a product like is not really present. From the research the team has done, there only exists one similar product -- called Multitronix -- that commercially available. The difference between that product and our product is the price. Our competitors' product price tag is in the thousands of dollars, while we have projected our control system to run anywhere between 200 to 300 dollars.

Goals and objectives of the company

The goals for the company is to be known within the model rocketry world. Many already well-established vendors already exist, so the company needs to make its presence known. This can be easily accomplished by attending rocket launches, and our sponsoring university rocketry programs like SCU's for example. A quantitative goal is to sell 100 units in the first year, and double that number the second year. This would give us a profit of about \$45,000 for the first two years. The team hopes that as production of the control system scales up, it will bring down the cost of the item, further increasing our profits. Another goal is to facilitate advances in aerospace engineering, and make young people interested in science and technology

Product Description

This product is an customizable controller that attaches to model rockets to effectively stabilize their trajectories. This product can be adjusted to the rocket diameter of the customer's choosing and must be calibrated to their needs. The final product would have a user friendly interface where they can turn it on before the flight and once the rocket is recovered, data can be retrieved from a MINI SD card and analyze in any computer.

Anybody who has ever flown a model rocket understands the limitations of small scale rockets i.e. wind disturbances that can cause a rocket to deviate from its vertical trajectory.

Therefore, this product is the perfect solution to anyone interested in stabilizing their flight actively and analyzing their flight data.

Potential markets

Another potential market for this product is the airplane model market. The team has learned that there are hobbyists out there who launch an RC plane that is attached to a rocket. Before the rocket reaches apogee, the RC plane detaches from the rocket and glides back to earth. In addition, many RC planes need some sort of control system in order to help stabilize the plane during maneuvers. The team plans to modify the existing control system to meet their needs.

Service or warranties

The product will have a guarantee on the software, but limited on the hardware. Because the canard fins will be sticking out of the body tube, it makes them vulnerable to damages after the rocket hits the ground. For example, the connecting shafts from the servos to the canard fins could become bent from the hit. Because of this, the product will have full warranty before the first flight is done, which means that if any component of the control system is not working properly then the customer can exchange it for a brand new one. After the control system has been flown, a limited warranty on the system is placed, which only includes the software.